Computational Geosciences (2022) 26:1345–1366
https://doi.org/10.1007/s10596-022-10165-3

ORIGINAL PAPER

Evaluating the impact of increasing temperatures on changes in Soil Organic Carbon stocks: sensitivity analysis and non-standard discrete approximation

Fasma Diele[1] · Ilenia Luiso[1] · Carmela Marangi[1] · Angela Martiradonna[2] · Edyta Woźniak[3]

Received: 30 July 2021 / Accepted: 15 July 2022 / Published online: 3 August 2022

Abstract

The *SOC change index*, defined as the normalized difference between the actual Soil Organic Carbon and the value assumed at an initial reference year, is here tailored to the RothC carbon model dynamics. It assumes as a baseline the value of the SOC equilibrium under constant environmental conditions. A sensitivity analysis is performed to evaluate the response of the model to changes in temperature, Net Primary Production (NPP), and land use soil class (forest, grassland, arable). A non-standard monthly time-stepping procedure has been proposed to approximate the SOC change index in the Alta Murgia National Park, a protected area in the Italian Apulia region, selected as a test site. The SOC change index exhibits negative trends for all the land use considered without fertilizers. The negative trend in the arable class can be inverted by a suitable organic fertilization program here proposed.

Keywords Soil Organic Carbon model · Sensitivity analysis · Non-standard discrete approximation

Mathematics Subject Classification (2010) 86A08 · 65L05 · 86-10 · 86-08

1 Introduction

For reporting on Target 15.1, one of the seventeen Sustainable Development Goals (SDGs) adopted by the United Nations [15] in 2015, the Good practice guidance [24] indicates how to calculate the extent of land degradation. It recommends the development and the use of analytical methods for measuring the three indicators which address the key aspects of land-based natural capital: trends in land cover, trends in land productivity and trends in soil organic carbon (SOC) stocks. These indicators can assess the quantity and the quality of land-based natural capital and most of the associated ecosystem services.

Roughly speaking, the SOC stock is the carbon captured by plants through photosynthesis which remains in the soil after the decomposition of soil organic matter. A decrease in SOC stocks is among the significant universal indicators for land and soil degradation and can compromise all the efforts to achieve the SDGs especially those with reference to food, health, water, climate, and land management [14].

Well-validated models which take into account the interactions among climate, soil and land use management can be used to predict SOC changes under the different management and climatic conditions. The Rothamsted carbon model (RothC, [3, 20]) is one of the most commonly used tools to simulate soil organic carbon dynamics in arable, grassland and forest systems. Although it does not place the action of bacteria at the heart of the mechanisms of decomposition as required by current theories [10, 13], it

✉ Fasma Diele
fasma.diele@cnr.it

Ilenia Luiso
i.luiso@ba.iac.cnr.it

Carmela Marangi
carmela.marangi@cnr.it

Angela Martiradonna
angela.martiradonna@uniba.it

Edyta Woźniak
ewozniak@cbk.waw.pl

1 Istituto per Applicazioni del Calcolo 'M.Picone', sede di Bari, Bari, Italy

2 Università degli Studi di Bari, Bari, Italy

3 Centrum Badań Kosmicznych Polskiej Akademii Nauk (CBK PAN), Warsaw, Poland

is widely used because it captures the general principles of soil organic dynamics, it is relatively simple and general, it requires relatively few parameters and can be easily applied at scales from regional [7], to global [17].

In this paper, for making a scenario analysis of SOC changes, we considered the evolution of the so-called *SOC change index* tailored to the RothC dynamics. It is defined as the difference between the SOC values at the last and the first year (as in [16]), here normalized by the carbon inputs generated by the total plant and the farmyard manure, both evaluated at the initial baseline year. As a test example, we evaluate the impact of changes in temperature on the achievement of land degradation neutrality for the SOC indicator in the Alta Murgia National Park, a protected area in the Apulia region located in the south of Italy. It is known that the increase or decrease of the SOC stocks under climate change will depend upon which process dominates, in the future and in a given location, between increased plant inputs through increases in net primary production (NPP), and increased decomposition rates [9]. With the aim of detecting factors which determine the size and the direction of change in the considered protected area, a sensitivity analysis, based on the direct method described in [4], is performed. The sensitivity analysis is applied to an ad hoc autonomous version of the RothC model where the time-dependent coefficients are replaced by constants equal to the coefficients averaged over a year. Our analysis provides local information on the impact of parameter changes on the behavior of the system solution. In particular, we evaluate the impact on the SOC change index of the variation of three representative parameters: mean annual temperature, NPP annual values with respect to reference values and degree of decomposability of plant material (the so-called *DPM/RPM ratio*), which in turn is related to the class of land use (forest, grassland and arable).

Trends in SOC changes from 2005, taken as the baseline year, to 2019, the final year, are simulated by means of a monthly discrete non-standard approximation of the continuous model for the forest, grassland and arable systems. It is based on the discrete non-standard monthly time-stepping procedure provided in [5] for solving the carbon dynamics in all of the compartments. Given the linearity of the RothC model, the SOC change can be discretized with the same matrix function of the monthly stepsize. Results obtained indicate negative trends for the SOC change in the case of forest, grassland and arable classes, considered without including the input of farm fertilizers. As a final result, we evaluate the optimal organic fertilization program to invert the negative trend of the arable class and keep positive the SOC change. When used with predicted climate and NPP data, the optimal fertilization program may guarantee the achievement of land degradation neutrality for the SOC indicator.

The paper is organized as follows. In Section 2 we briefly describe the original RothC model and define the SOC indicator for the continuous counterpart of the original model. Moreover, we introduce a more realistic representation of the density function of the plant carbon input which can be proven to be periodic. Input data and parameters are then identified and described. In Section 3 we explain how the issue of determining the initial carbon input is solved in the proposed formulation and we define a SOC change index which overcomes the problem. Then, in Section 4 we describe the SOC change index dynamics and, in Section 5 we determine the sensitivity of the model to the variation of temperature, NPP and land use class. The issue of a possible positive contribution of organic fertilization is faced in Section 6 where we propose to consider the farmyard manure input as a control variable to reach neutrality. To perform the simulations, we apply a numerical non-standard technique which preserves the equilibrium state of the continuous dynamics and is described in Section 7. In Section 8 we present a test case illustrating the trends of SOC change in a protected area, in the years 2005–2019, as a function of the measured changes in temperature and NPP for the three land use classes analyzed (forest, grassland, arable). Finally, in Section 9 we draw our conclusions.

2 The RothC model

Within the RothC model, soil organic carbon is divided into the five carbon pools noted: c_{dpm}, c_{rpm}, c_{hum}, c_{bio} and c_{iom} (see Fig. 1). The already decomposed plant material is regarded as c_{hum}, whereas the total carbon mass of microbial organisms is represented by the c_{bio} pool. All non decomposable or inert material is defined as c_{iom}. In general, all pools c_i will decompose and form CO_2, c_{bio} and c_{hum}. The four active compartments c_{dpm}, c_{rpm}, c_{hum} and c_{bio}, undergo decomposition as a function of different rate constants which correspond to the entries of the vector $\mathbf{k} = [k_{dpm}, k_{rpm}, k_{bio}, k_{hum}]^\intercal$, and of the rate modifier $\rho(t)$ which depends on the clay content of the soil, on climate variables (rainfall, temperature, open pan evaporation) and land cover. The fraction $\alpha + \beta$ of metabolised carbon incorporated into the sum of compartments $c_{bio}(t) + c_{hum}(t)$ is determined by the clay content of the soil, while the remaining part $\delta := 1 - \alpha - \beta$ is released as CO_2 and lost by the system.

For the aim of what follows we denote with $T > 0$ the length of a reference time interval (generally one year) and we formulate the RothC model as:

$$\frac{d\mathbf{c}}{dt} = \rho(t)\, A\, \mathbf{c} + \mathbf{b}(t), \qquad t \in]\, t_0 + nT,\ t_0 + (n+1)T\,], \quad n = 0, \ \ldots, \tag{1}$$

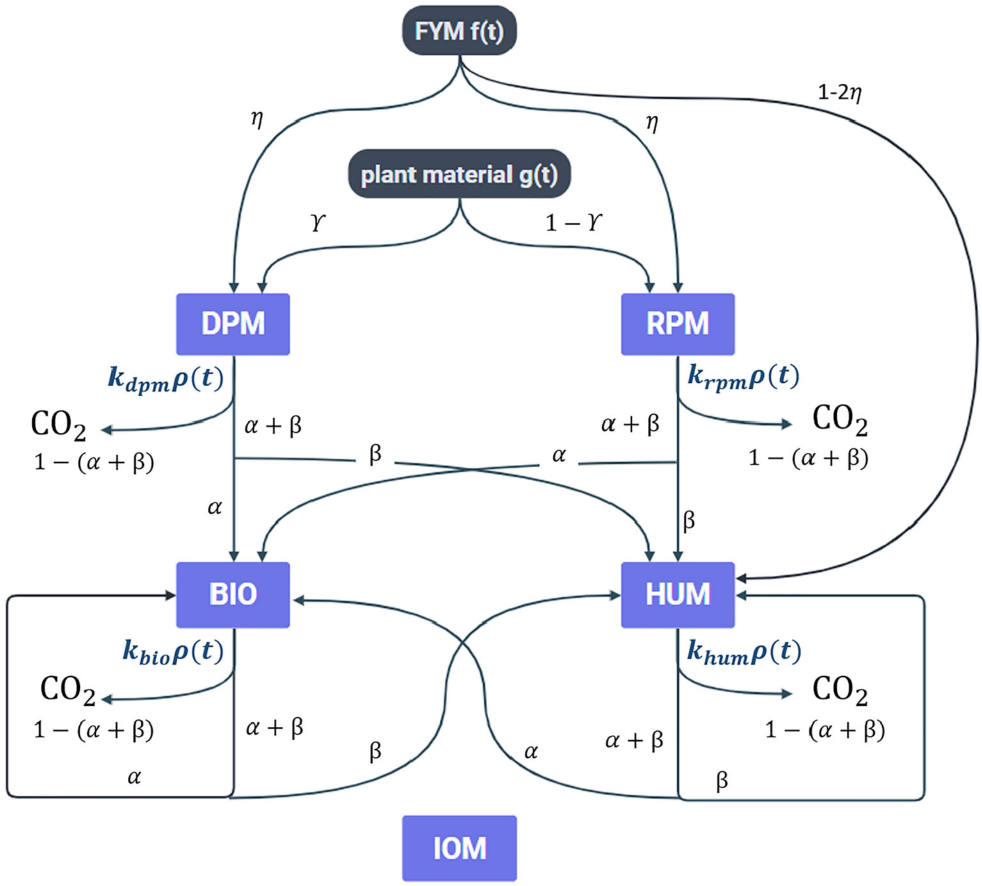

Fig. 1 Flow chart of the RothC model

where $\mathbf{c}(t) = [c_{dpm}(t), c_{rpm}(t), c_{bio}(t), c_{hum}(t)]^\intercal$ and $\mathbf{c}(t_0) = \mathbf{c}_0 \geq 0$ denotes the vector of the initial concentrations. The matrix A is given by

$$A = \begin{pmatrix} -k_{dpm} & 0 & 0 & 0 \\ 0 & -k_{rpm} & 0 & 0 \\ \alpha\, k_{dpm} & \alpha\, k_{rpm} & (\alpha-1)\, k_{bio} & \alpha\, k_{hum} \\ \beta\, k_{dpm} & \beta\, k_{rpm} & \beta\, k_{bio} & (\beta-1)\, k_{hum} \end{pmatrix}.$$

The vector $\mathbf{b}(t)$ represents the carbon amount entering the system at time t. It takes into account both the input of plant residues $g(t)\,\mathbf{a}^{(g)}$ and the input of farmyard manure (FYM) $f(t)\,\mathbf{a}^{(f)}$, so that

$$\mathbf{b}(t) := g(t)\,\mathbf{a}^{(g)} + f(t)\,\mathbf{a}^{(f)}.$$

The entries of vectors $\mathbf{a}^{(g)} := [\gamma,\ 1-\gamma,\ 0,\ 0]^\intercal$ and $\mathbf{a}^{(f)} := [\eta,\ \eta,\ 0,\ 1-2\,\eta]^\intercal$ are the fraction inputs $0 \leq \gamma \leq 1$, $0 \leq \eta \leq 1/2$, which sum up to 1.

Definition 1 We define as SOC indicator of the continuous RothC model (1) the function $SOC(t) = c_{iom}(t) + c_{dpm}(t) + c_{rpm}(t) + c_{bio}(t) + c_{hum}(t)$ for $t \geq t_0$, where c_{iom} denotes the constant carbon content in the inactive compartment IOM.

Although different approaches can be adopted for calculating the size of IOM, [19, 21], here we use the classical equation given by Falloon et al. in [6]:

$$c_{iom}(t) = 0.049\, SOC^{1.139}(t)$$

so that the SOC indicator is obtained by solving the equation

$$0.049\, SOC^{1.139}(t) - SOC(t) + soc(t) = 0,$$

where

$$soc(t) := c_{dpm}(t) + c_{rpm}(t) + c_{bio}(t) + c_{hum}(t) \qquad (2)$$

satisfies the differential equation

$$\frac{dsoc}{dt}(t) = \mathbb{1}^\intercal \frac{d\mathbf{c}}{dt}(t) = \rho(t)\,\mathbb{1}^\intercal A\,\mathbf{c} + g(t) + f(t)$$
$$= -\rho(t)\,\delta\,\mathbf{k}^\intercal\mathbf{c} + g(t) + f(t). \quad (3)$$

2.1 A realistic representation of $g(t)$

Towards a realistic analytic representation of the density function $g(t)$ of plant carbon input, we consider that $g(t)$ can be represented as follows

$$g(t) = P(t_0 + n\,T)\ \hat{g}(t) \qquad \forall t \in [t_0 + nT, t_0 + (n+1)T],$$
$$n = 0,\ \ldots, \qquad (4)$$

where

$$\hat{g}(t) := \frac{g(t)}{\int_{t_0+nT}^{t_0+(n+1)T} g(s)\, ds}. \tag{5}$$

The function $\hat{g}$ represents the density distribution of plant carbon inputs into the soil expressed as a proportion of the total $P(t_0 + nT) := \int_{t_0+nT}^{t_0+(n+1)T} g(s)\, ds$, in each time interval $[t_0 + nT,\ t_0 + (n+1)T]$ of length T, for $n = 0, 1, \ldots$. In real applications the function $\hat{g}(t)$ is known and, as it depends only on seasonality, it is well represented by an annual periodic function. We have the following result.

Theorem 1 *Set $T > 0$ and suppose that $g(t)$ is a positive function which satisfies the following property*

$$g(t + T) = g(t)\, \frac{\int_{t_0+(n+1)T}^{t_0+(n+2)T} g(s)\, ds}{\int_{t_0+nT}^{t_0+(n+1)T} g(s)\, ds},$$

for all $t \in [t_0+nT,\ t_0+(n+1)T]$, and $n = 0, 1, \ldots$. Then, the function $\hat{g}(t)$, defined in Eq. 5, *satisfies $0 < \hat{g}(t) < 1$, results periodic with period T and $\int_{t_0}^{t_0+T} \hat{g}(s)\, ds = \int_{t_0+nT}^{t_0+(n+1)T} \hat{g}(s)\, ds = 1$, for all $n = 0, 1 \ldots$.*

Proof The result trivially follows by observing that if $t \in [t_0+nT,\ t_0+(n+1)T\,[$, then $t + T \in [t_0+(n+1)T,\ t_0+(n+2)T\,[$. Consequently,

$$\hat{g}(t+T) = \frac{g(t + T)}{\int_{t_0+(n+1)T}^{t_0+(n+2)T} g(s)\, ds} = \hat{g}(t),$$

for all $t \in [t_0 + nT,\ t_0 + (n+1)T\,]$ and $n = 0, 1, \ldots$. □

2.2 Input data and parameters

Let us identify all the input data necessary to the RothC dynamics.

- Input per unit time (*month*) of plant residues $g(t)$ $[t\, C\, ha^{-1}\, month^{-1}]$ and farmyard manure $f(t)[t\, C\, ha^{-1}\, month^{-1}]$, if any.
  The function $g(t)$ is supposed to be expressed as in Eq. 4. By means of Net Primary Production (NPP), it is possible to estimate

$$P(t_0+nT) = P(t_0 + (n-1)\,T)\, \frac{NPP(t_0 + nT)}{NPP(t_0 + (n-1)\,T)} = P(t_0)\, N_P^{(n)} \qquad \forall n = 1, 2 \ldots \tag{6}$$

  the total plant carbon input in the year $[t_0+nT,\ t_0+(n+1)T]$, where $N_P^{(n)} := \frac{NPP(t_0 + nT)}{NPP(t_0)}$. The function $\hat{g}(t) = \hat{g}_r(t)$ is supposed annual periodic and assuming different known shapes according to the land use.
- clay content of the soil cly (as a percentage);
- r the degree of decomposability of incoming plant material, i.e. the *DPM over RPM ratio*;
- air temperature $Temp(t)$ [°C], rainfall $rain(t)\,[mm]$, potential evapotranspiration[1] $pet(t)$. In our tests $pet(t)$ is estimated from weather data by means of Thornthwaite's formula (see Appendix).
- $\mathbf{c}(t_0)\,[\,t\, C\, ha^{-1}]$ the vector of the initial concentrations sampled at a soil layer of depth $d\,[cm]$.

Let us identify all the parameters involved in the RothC dynamics.

- $A = A(\alpha, \beta, \mathbf{k})$. From the clay content, we can evaluate the *Soil Texture Factor* according to $x = 1.67\,(1.85 + 1.60\, e^{-0.0786\, cly})$, and consequently $\alpha = \frac{0.46}{x+1}$ and $\beta = \frac{1}{x+1} - \alpha$; the entries of $\mathbf{k}$ are given by $k_{dpm} = 10/T\,[time^{-1}]$, $k_{rpm} = 0.3/T\,[time^{-1}]$, $k_{bio} = 0.66/T\,[time^{-1}]$, $k_{hum} = 0.02/T\,[time^{-1}]$.
- $\mathbf{b}(t) = \mathbf{b}(t, \gamma, \eta)$. Here $\eta = 0.49$ while $\gamma(r) = \frac{r}{r+1}$ varies according to the land use. Values $0 < r < 0.5$ of DPM over RPM ratio are associated to the *forest* class, $0.5 \le r < 1$ to the *grassland* class, $r \ge 1$ to the *arable* class.
- $\rho(t) = k_a(Temp(t))\; k_b\,(Acc(rain(t),\ M(cly, d))\; k_c(t, r)$.
  The modifying factor related to the temperature is generalized with respect to the original given in [3], in order to assume a value equal to 1 in correspondence of the mean annual temperature $Temp^{(0)}$ in the interval $[\,t_0,\ t_0 + T\,[$, i.e.

$$k_a(Temp(t)) := \frac{47.91}{1 + e^{\frac{106.06}{Temp(t) + 106.06/log(46.91) - Temp^{(0)}}}},$$

  so that $k_a(Temp^{(0)}) = 1$.
  The factor $k_c(t, r)$, associated to the soil cover,

$$k_c(t, r) = \begin{cases} 0.6 & 0 < r < 1 \\ S_r(t) & r \ge 1, \end{cases}$$

  with $S_r(t) = S_r(t + T)$ assuming values between 0.6 in the periods of the year when soil is vegetated and the maximum value 1, when bare.

[1] The original model uses open pan evaporation; here the model is used in a modified version which makes use of potential evapotranspiration

The maximum soil moisture deficit M and the point at which respiration (i.e. microorganism activity) begins to slow M_b, are defined as $M := M(cly, d) = -(20 + 1.3\,cly - 0.01\,cly^2)\,\frac{d}{23}$ and $M_b = 0.444\,M$. The accumulated soil moisture deficit $Acc(t, M)$ is calculated from the first time in $[t_0 + nT, t_0 + (n+1)T]$ where evaporation $pet(t)$ exceeds rainfall the maximum soil moisture deficit M. When there is more rainfall than evaporation, the soil will start to wet up.

The rate modifying factor for moisture varies between 0.2 and 1 as follows

$$k_b(Acc(t, M)) := \begin{cases} 0.2+(1-0.2)\dfrac{M-Acc(t,M)}{M-M_b} & Acc(t,M) < M_b \\ 1 & \text{otherwise.} \end{cases}$$

3 Determining the initial plant inputs

In all practical applications, RothC is run in 'reverse mode' to calculate the initial plant inputs to the soil for the given environmental conditions. The underlying hypothesis is that the observed carbon stocks correspond to a stable constant or annual periodically varying long-term solution for their dynamics. Once the initial plant inputs have been established in this way, in order to simulate future scenarios, changes in NPP [25], in climate conditions, or in land use will determine changes in predicted carbon stocks.

Under the hypothesis that the observed carbon stocks correspond to their values at a stable equilibrium, we are going to illustrate how it is possible to avoid the first run in 'reverse mode' to calculate the initial plant inputs. After setting a monitoring temporal interval $[t_0 + T, T_f]$, by following the approach indicated in [15], the baseline of SOC indicator against which Land Degradation Neutrality is to be achieved, is supposed to correspond to the carbon stocks equilibrium for averaged values of temperature, accumulate soil moisture deficit, and soil cover in a period $[t_0, t_0 + T]$ immediately prior the monitoring time interval.

As concerns the average value for the factor $k_c(t, r)$ associated to the soil cover, it can be approximated as follows:

$$\overline{k_c(r)} = \begin{cases} 0.6 & 0 \le r < 1 \\ \displaystyle ⨍_{t_0}^{t_0+T} S_r(s)ds \approx 0.6 + \frac{N_b}{30} & r \ge 1, \end{cases}$$

where $0 \le N_b \le 12$ (generally $N_b = 4$, see e.g. [25]) is the number of months per year of bare soil for arable class.

In order to have a smooth dependence on r, we approximate $\overline{k_c(r)}$ with the $\mathcal{C}^\infty$-function

$$\begin{aligned} k_c(r) &:= 0.6 + \frac{N_b}{30}\frac{e^{x(r)}}{1+e^{x(r)}}, \\ x(r) &:= \frac{30(r-1)}{r} \qquad r > 0. \end{aligned} \tag{7}$$

The function $k_c(r)$ for a generic crop related to $N_b = 4$ bare months per year, is illustrated in Fig. 2.

Denoting with $Temp^{(0)}$ and $Acc^{(0)}$ the averaged values for temperature and accumulated soil deficit on the period $[t_0, t_0+T]$ assumed as reference interval, then the modifying factor $\rho(t)$ is approximated by $\rho^{(0)}(r) := k_b(Acc^{(0)})k_c(r)$, as $k_a(Temp^{(0)}) = 1$.

Setting $F(t_0) = \int_{t_0}^{t_0+T} f(s)ds$, then the model (1), can be written as

$$\frac{d\mathbf{c}}{dt} = \rho^{(0)}(r)A\mathbf{c} + \frac{P(t_0)}{T}\mathbf{a}^{(g)} + \frac{F(t_0)}{T}\mathbf{a}^{(f)}, \qquad t \in]t_0, t_0+T]. \tag{8}$$

Suppose that $\mathbf{c}(t_0)$ i.e. the distribution of the measured $SOC(t_0)$ among compartments is known and satisfies

$$0.049SOC^{1.139}(t_0) - SOC(t_0) + \mathbb{1}^\intercal\mathbf{c}(t_0) = 0.$$

We assume that $\mathbf{c}(t_0)$ is equal to the equilibrium of the dynamical system (8), i.e.

$$\mathbf{c}(t_0) = -\frac{1}{T\rho^{(0)}(r)}A^{-1}\left(P(t_0)\mathbf{a}^{(g)} + F(t_0)\mathbf{a}^{(f)}\right). \tag{9}$$

Consequently,

$$\begin{aligned} P(t_0)\mathbf{a}^{(g)} &= -T\rho^{(0)}(r)A\mathbf{c}(t_0) - F(t_0)\mathbf{a}^{(f)} \\ P(t_0) + F(t_0) &= -T\rho^{(0)}(r)\mathbb{1}^\intercal A\mathbf{c}(t_0) = T\rho^{(0)}(r)\delta\mathbf{k}^\intercal\mathbf{c}(t_0). \end{aligned} \tag{10}$$

Under the hypothesis that $F(t_0)$ is known (i.e. the amount of the total farmyard manure used in the interval $[t_0, t_0 + T]$), it follows that the initial plant inputs to the soil is given by

$$\begin{aligned} P(t_0) = T\rho^{(0)}(r)\delta\,(&k_{dpm}c_{dpm}(t_0) + k_{rpm}c_{rpm}(t_0) \\ &+ k_{bio}c_{bio}(t_0) + k_{hum}c_{hum}(t_0)) - F(t_0). \end{aligned} \tag{11}$$

Then, for all $n = 1, 2\ldots$ the system

$$\begin{aligned} &\frac{d\mathbf{c}}{dt}(t) = \rho(t)A\mathbf{c} + P(t_0 + nT)\hat{g}_r(t)\mathbf{a}^{(g)} + f(t)\mathbf{a}^{(f)} \\ &P(t_0 + nT) = P(t_0)N_P^{(n)} \end{aligned} \tag{12}$$

is solved for $t \in]t_0 + nT, t_0 + (n+1)T]$ starting from $\mathbf{c}(t_0 + T) = \mathbf{c}(t_0)$ given in Eq. 9 and $P(t_0)$ given in Eq. 11, until $t_0 + (n+1)T \le T_f$.

Fig. 2 The rate constant modifying factor k_c as a smooth function of DPM/RPM ratio

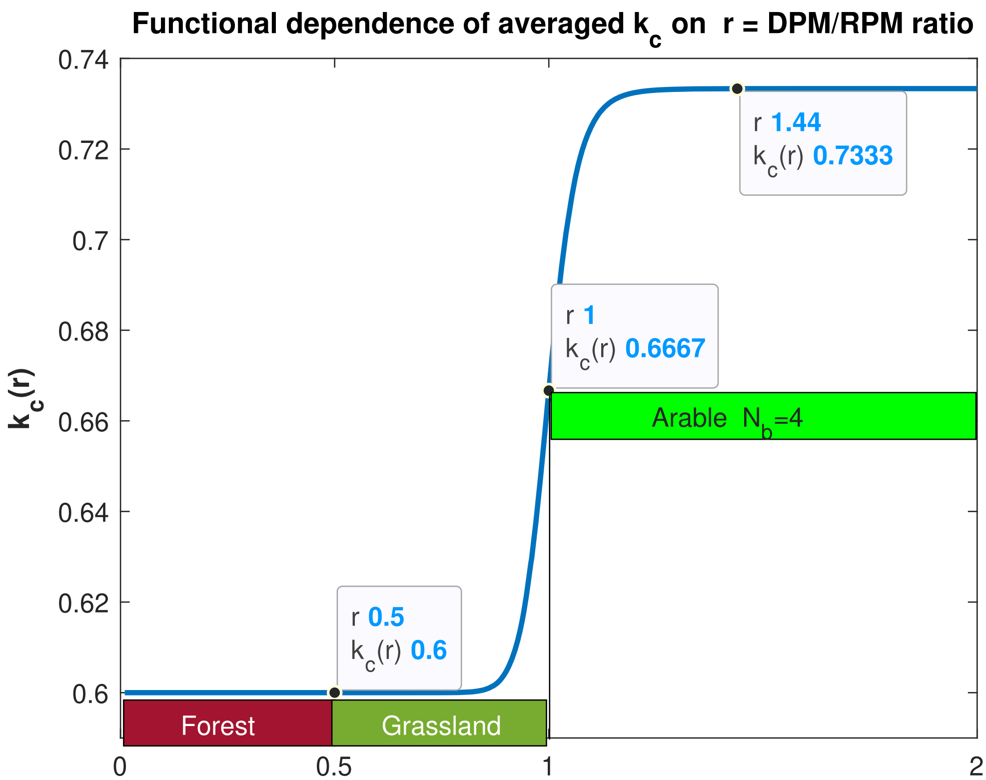

4 The dynamics of the SOC change index

Soil organic carbon dynamics are driven by changes in climate and land cover or land use. In natural ecosystems, the balance of SOC is determined by gains, through plant and other organic inputs, and losses, due to the organic matter turnover [25]. Globally, under a warming climate, increases are seen both in carbon inputs to the soil due to higher NPP, and in SOC losses due to increased decomposition. The balance between these processes defines the SOC change. In some regions the processes balance, but in others, one process is affected by climate more than the other.

For making a scenario analysis of SOC change, which does not depend on the specific initial measured SOC value but only on the hypothesis of an initial environmental equilibrium, a useful tool is given by the *SOC change index* defined as the variable of change of carbon stocks normalized as follows.

Definition 2 We indicate with $\Delta soc(t)$ the *SOC change index* defined as $\Delta soc(t) := \dfrac{soc(t) - soc(t_0)}{P(t_0) + F(t_0)}$ with $soc(t) := \mathbb{1}^\intercal \mathbf{c}(t)$, where $\mathbf{c}(t)$ solves Eq. 12 and $P(t_0) + F(t_0)$ is given in Eq. 10.

Notice that the sign of the index $\Delta soc(t)$ detects if, at the time t, the sum of soil carbon contained in compartments is greater than its initial value. In what follows, for detecting changes in SOC stock in a specific area, we deduce its temporal dynamics.

Theorem 2 *Under the hypothesis that* $P(t_0) + F(t_0) > 0$, *the dynamics of the variable*

$$\Delta\mathbf{c}(t) := \frac{\mathbf{c}(t) - \mathbf{c}(t_0)}{P(t_0) + F(t_0)}, \quad t \in [t_0 + nT, t_0 + (n+1)T],$$
$$n = 1, 2, \dots,$$

is governed by the equation

$$\begin{aligned} \frac{d\Delta\mathbf{c}}{dt} &= \rho(t) A \Delta\mathbf{c} + \left(N_P^{(n)} \hat{g}_r(t) - \frac{\rho(t)}{T\rho^{(0)}(r)} \right) \xi \mathbf{a}^{(g)} \\ &\quad - \frac{\rho(t)}{T\rho^{(0)}(r)} (1 - \xi) \mathbf{a}^{(f)} + \frac{f(t)}{P(t_0) + F(t_0)} \mathbf{a}^{(f)}, \\ &\quad \Delta\mathbf{c}(t_0 + T) = \Delta\mathbf{c}(t_0) = \mathbf{0}, \end{aligned} \tag{13}$$

where $0 \le \xi := \dfrac{P(t_0)}{P(t_0) + F(t_0)} \le 1$.

Notice that when the value $\xi = 0$ then the initial plant carbon input $P(t_0) = 0$; while $\xi = 1$ corresponds to the case $F(t_0) = 0$. Hence, by increasing ξ from 0 to 1, we explore all the cases from only-farmyard manure initial carbon input to only-plant initial carbon input.

The dynamics for $\Delta soc(t)$ can be immediately deduced from the dynamics of $\Delta\mathbf{c}(t)$ as follows.

Corollary 1 *In case of farmyard manure input, the dynamics of the SOC change index $\Delta soc(t)$ for $t \in [t_0 + nT, t_0 + (n+1)T]$, for $n = 1, 2, \ldots$, is governed by the equation*

$$\frac{d\Delta soc(t)}{dt} = -\delta\rho(t)\mathbf{k}^{\mathsf{T}}\Delta\mathbf{c} + \xi N_P^{(n)}\hat{g}_r(t) - \frac{\rho(t)}{T\rho^{(0)}(r)} + \frac{f(t)}{P(t_0)+F(t_0)}, \tag{14}$$

where $\Delta\mathbf{c}(t)$ solves Eq. 13 *and $\Delta soc(t_0 + T) = \Delta soc(t_0)$* $= 0$.

Remark 1 Notice that, whenever farmyard manure amendments are not considered at all, specific results can be deduced from Theorem 2 and Corollary 1 by setting $f(t) = 0$ for all $t \geq t_0$ and noticing that $F(t_0) = 0$ implies $\xi = 1$.

As a consequence of the above remark, for all scenarios that do not consider fertilization actions, e.g. forest or (not-improved) grassland land use classes, the dynamics of the SOC change index in Eqs. 14–13 do not depend on the value $P(t_0) + F(t_0) = P(t_0)$. It follows that, for those scenarios, our model is able, differently from the classical RothC model (12), to provide the crucial information about the sign of SOC change, even in absence of $P(t_0)$ and $\mathbf{c}(t_0)$ values. Indeed, $\Delta soc(t)$ variable has the same sign of the SOC change since $\Delta soc(t) := \dfrac{soc(t) - soc(t_0)}{P(t_0)}$ with $P(t_0) > 0$. We underline that establishing the sign of the SOC change with respect to an initial baseline value, whatever it is, has a crucial importance in the context of a LDN analysis [18].

5 Sensitivity of the SOC change index to parameters

In this section, we want to study the relative importance of the different factors responsible for changes in SOC stock. This will be done throughout a sensitivity analysis of the SOC change index related to the dependence on the temperature, NPP and the class of land use, under the hypothesis of no fertilization amendments. We will make use of the direct method in [4] where the analysis of sensitivity is local and described by first-order derivatives. Notice that, for a better reading, the results of this section are given without proofs which can be found in Appendix.

In this setting, $\phi \in \mathbb{R}$ is a parameter affecting the dynamics $\dfrac{d\mathbf{y}}{dt} = \mathbf{f}(\mathbf{y}(t,\phi),\phi)$ of the n-dimensional variable $\mathbf{y}(t)$. The direct method requires the integration of an additional set of differential equations, together with the original system, to obtain the vector of sensitivities $\mathbf{s}_{\mathbf{y},\phi}(t)$, whose components are defined as $\dfrac{\partial y_i(t,\phi)}{\partial\phi}$, i.e.

$$\begin{aligned} &\frac{d\mathbf{y}}{dt} = \mathbf{f}(\mathbf{y}(t,\phi),\phi), \qquad \mathbf{y}(t_0,\phi) = \mathbf{y}_0(\phi) \\ &\frac{d\mathbf{s}_{\mathbf{y},\phi}}{dt}(t,\phi) = \frac{\partial\mathbf{f}}{\partial\phi}(\mathbf{y}(t,\phi),\phi) + \frac{\partial\mathbf{f}}{\partial\mathbf{y}}(\mathbf{y}(t,\phi),\phi)\,\mathbf{s}_{\mathbf{y},\phi}(t), \\ &\mathbf{s}_{\mathbf{y},\phi}(t_0) = \frac{\partial\mathbf{y}_0(\phi)}{\partial\phi}, \end{aligned} \tag{15}$$

where $\dfrac{\partial\mathbf{f}}{\partial\mathbf{y}}$ denotes the Jacobian matrix of $\mathbf{f}$.

In order to apply the above described direct method, we need to replace non-autonomous dynamics with autonomous ones. We focus on the case when $f(t) = 0$ for all $t \geq t_0$; moreover, as our sensitivity analysis is local, the approximated autonomous system is derived only in the first year.

Let us come back to the equation for $\Delta\mathbf{c}(t)$ in Theorem 2 in case when $f(t) = 0$

$$\frac{d\Delta\mathbf{c}}{dt} = \rho(t)A\Delta\mathbf{c} + \left(N_P^{(n)}\hat{g}_r(t) - \frac{\rho(t)}{T\rho^{(0)}(r)}\right)\mathbf{a}^{(g)}. \tag{16}$$

At first, we replace $Temp(t)$ and $Acc(t)$ with their averaged values, $Temp^{(1)}$ and $Acc^{(1)}$ in the interval $]t_0 + T, t_0 + 2T]$ so that $\rho(t)$ can be approximated by $\rho^{(1)}(r) := k_a(Temp^{(1)})k_b(Acc^{(1)})k_c(r)$, where $k_c(r)$ is given in Eq. 7. As $\displaystyle\int_{t_0+T}^{t_0+2T}\hat{g}_r(s)ds = \frac{1}{T}$, we define the autonomous counterpart of the model (16) in the first year as follows:

$$\frac{d\Delta\bar{\mathbf{c}}}{dt} = \rho^{(1)}(r)A\Delta\bar{\mathbf{c}} + \vartheta^{(1)}\mathbf{a}^{(g)}, \quad \Delta\bar{\mathbf{c}}(t_0 + T) = \mathbf{0}, \tag{17}$$

for $t \in]t_0 + T, t_0 + 2T]$, where[2]

$$\vartheta^{(1)} := \frac{1}{T}\left(N_P^{(1)} - \frac{\rho^{(1)}(r)}{\rho^{(0)}(r)}\right), \tag{18}$$

whose solution is given by

$$\Delta\bar{\mathbf{c}}(t) = (t-t_0-T)\vartheta^{(1)}\varphi\left((t-t_0-T)\rho^{(1)}(r)A\right)\mathbf{a}^{(g)}, \tag{19}$$

where

$$\varphi(z) := z^{-1}(e^z - 1). \tag{20}$$

A formal derivation of the above approximation is given by the following theorem.

Theorem 3 *The solution $\Delta\bar{\mathbf{c}}(t)$ of the autonomous system (17) approximates the solution of the non-autonomous*

[2]Let us observe that $\vartheta^{(1)}$ does not depend on r, in fact $\vartheta^{(1)} = \frac{1}{T}\left(N_P^{(1)} - \frac{k_a(Temp^{(1)})k_b(Acc^{(1)})}{k_b(Acc^{(0)})}\right)$.

system $\Delta\mathbf{c}(t)$ *in* Eq. 16 *in a right neighborhood of* $t_0 + T$ *of length* $\epsilon < T$. *In fact*

$$\Delta\bar{\mathbf{c}}(t) - \Delta\mathbf{c}(t) = \epsilon\left(\vartheta^{(1)}\varphi\left(B(\epsilon)\right) - \vartheta(t_0+T)I\right)\mathbf{a}^{(g)} + \mathbf{O}(\epsilon^2),$$

where $\vartheta(t) := \left(N_P^{(1)}\hat{g}_r(t) - \dfrac{\rho(t)}{T\rho^{(0)}}\right)$ *and the matrix* $B(\epsilon) := \epsilon\rho^{(1)}(r)A$ *is negative definite. Moreover, there is a norm on* $\mathbb{R}^4$ *and a constant* $c > 0$ *such that* $\|\varphi(B(\varepsilon))\| < 1$ *and* $\|\mathbf{a}^{(g)}\| < c$*, therefore the leading error term can be bounded as follows*

$$\left\|\left(\vartheta^{(1)}\varphi\left(B(\epsilon)\right) - \vartheta(t_0+T)I\right)\mathbf{a}^{(g)}\right\| \le 2c\max(|\vartheta^{(1)}|, |\vartheta(t_0+T)|).$$

With the previous notations, we define:

Definition 3 The *sensitivity of the SOC change index to the parameter* ϕ is defined as the sum of the entries of the vector $\mathbf{s}_{\Delta\bar{\mathbf{c}},\phi}$, which is the sensitivity to the parameter ϕ of the variable $\Delta\bar{\mathbf{c}}(t)$, whose dynamics is described in Eq. 17.

In the following, we are going to analyze the sensitivity of the SOC change index to three different parameters: $Temp^{(1)}$ representing the annual averaged temperature, $N_P^{(1)} := NPP(t_0+T)/NPP(t_0)$ representing the NPP input normalized by the value at the reference year, and r related to change of land use, from forest (lowest values of r) to arable (highest value of r).

5.1 Sensitivity of the SOC change index to the parameter *Temp*$^{(1)}$

Accordingly to Definition 3, we define the sensitivity of the SOC change index to $Temp^{(1)}$ the quantity $s_{\Delta soc,Temp^{(1)}} := \mathbb{1}^{\mathsf{T}}\mathbf{s}_{\Delta\bar{\mathbf{c}},Temp^{(1)}}$. The following theorem holds.

Theorem 4 *The sensitivity of the SOC change index to* $Temp^{(1)}$ *satisfies the following differential equation*

$$\frac{ds_{\Delta soc,Temp^{(1)}}}{dt} = -\rho^{(1)}(r)\delta\mathbf{k}^{\mathsf{T}}\mathbf{s}_{\Delta\bar{\mathbf{c}},Temp^{(1)}} - \frac{\partial\rho^{(1)}(r)}{\partial Temp^{(1)}}\left(\delta\mathbf{k}^{\mathsf{T}}\Delta\bar{\mathbf{c}} + \frac{1}{T\rho^{(0)}(r)}\right) \quad (21)$$

for $t \in]t_0+T, t_0+2T]$*, with the initial condition*

$$s_{\Delta soc,Temp^{(1)}}(t_0+T) = 0.$$

Moreover, there exists an $\epsilon > 0$ *such that for all* $t \in [t_0+T, t_0+T+\epsilon]$

$$s_{\Delta soc,Temp^{(1)}}(t) \le 0.$$

Remark 2 For sufficiently small values of t, the sensitivity of the SOC change index to $Temp^{(1)}$ is a negative function of time. Consequently, an initial increase in annual averaged temperature $Temp^{(1)}$ decreases the null initial value of Δsoc. Recalling that the sign of the index $\Delta soc(t)$ detects if at the time t the sum of soil carbon contained in compartments is greater than its initial value, we conclude that an initial increase in annual averaged temperature $Temp^{(1)}$ has a negative effect on the achievement of land degradation neutrality.

5.2 Sensitivity of the SOC change index to the $N_P^{(1)}$ ratio

According to Definition 3, the sensitivity of the SOC change index to $N_P^{(1)}$ is given by $s_{\Delta soc,N_P^{(1)}} := \mathbb{1}^{\mathsf{T}}\mathbf{s}_{\Delta\bar{\mathbf{c}},N_P^{(1)}}$. The following theorem holds.

Theorem 5 *The sensitivity of the SOC change index to* $N_P^{(1)}$ *satisfies the following initial value problem*

$$\frac{ds_{\Delta soc,N_P^{(1)}}}{dt} = -\rho^{(1)}(r)\delta\mathbf{k}^{\mathsf{T}}\mathbf{s}_{\Delta\bar{\mathbf{c}},N_P^{(1)}} + \frac{1}{T},$$
$$t \in]t_0+T, t_0+2T]$$
$$s_{\Delta soc,N_P^{(1)}}(t_0+T) = 0. \quad (22)$$

Moreover, $s_{\Delta soc,N_P^{(1)}}(t) \ge 0$ *for all* $t \in [t_0+T, t_0+2T]$.

Remark 3 The sensitivity of the SOC change index to $N_P^{(1)}$ is positive, consequently an increase of the $N_P^{(1)}$ ratio increases the null initial value of Δsoc. Recalling that the sign of the index $\Delta soc(t)$ detects if at the time t the sum of soil carbon contained in compartments is greater than its initial value, we conclude that an increase in annual NPP values has a positive effect on the achievement of land degradation neutrality.

5.3 Sensitivity of the SOC change index to the parameter *r*

According to Definition 3, the sensitivity of the SOC change index to r is given by $s_{\Delta soc,r} := \mathbb{1}^{\mathsf{T}}\mathbf{s}_{\Delta\bar{\mathbf{c}},r}$. The following theorem holds.

Theorem 6 *The sensitivity of the SOC change index to* r *satisfies the following initial value problem*

$$\frac{ds_{\Delta soc,r}}{dt} = -\rho^{(1)}(r)\delta\mathbf{k}^{\mathsf{T}}\mathbf{s}_{\Delta\bar{\mathbf{c}},r} - \frac{\partial\rho^{(1)}(r)}{\partial r}\delta\mathbf{k}^{\mathsf{T}}\Delta\bar{\mathbf{c}}$$
$$s_{\Delta soc,r}(t_0+T) = 0, \quad (23)$$

for $t \in]t_0+T, t_0+2T]$*. Moreover, if* $\vartheta^{(1)}$ *is positive, then there exists an* $\epsilon > 0$ *such that* $s_{\Delta soc,r}(t) \le 0$ *for all*

$t \in [t_0+T, t_0+T+\epsilon]$. *Conversely, if* $\vartheta^{(1)}$ *is negative, then there exists an* $\epsilon > 0$ *such that* $s_{\Delta soc,r}(t) \geq 0$ *for all* $t \in [t_0+T, t_0+T+\epsilon]$.

Remark 4 For sufficiently small values of t, the sensitivity of the SOC change index to r has the opposite sign of $\vartheta^{(1)}$. This means that an initial increase in the parameter r increases or decreases the null initial value of Δsoc accordingly to negative or positive values of $\vartheta^{(1)}$. More in details, when changes in temperature increase the annual value of the NPP more then the modifying factor $\rho^{(1)}(r)$, both with respect to their initial values i.e. $\frac{NPP(t_0+T)}{NPP(t_0)} \leq \frac{\rho^{(1)}(r)}{\rho^{(0)}(r)}$, this positively impacts all land use classes; vice versa, when changes in temperature increase the modifying factor $\rho^{(1)}(r)$ more then the annual value of the NPP with respect to their initial value i.e. $\frac{NPP(t_0+T)}{NPP(t_0)} > \frac{\rho^{(1)}(r)}{\rho^{(0)}(r)}$, then SOC change negatively impacts all the land use class. In both positive and negative case the arable land use class results to be the most affected.

6 Increasing SOC in arable with farmyard manure amendments

To achieve SOC neutrality it is necessary to implement land-based mitigation solutions that sequester large amounts of CO_2 from the atmosphere [12]. For instance, this can be done by enhancing the natural sink of carbon via reforestation, through bioenergy cultivation with carbon capture and storage, and via carbon sequestration in agricultural soils through improved management practices [8]. Agricultural soils are markedly SOC-depleted as a consequence of cultivation because the continuous harvesting of plants reduces the amount of plant litter that is returned to the soil. The addition of carbon input is the best option to increase SOC stocks in agricultural soils [2] and, for croplands, this can be achieved with recommended management practices based, for example, on the use of crop species and varieties that have a greater root mass or the use of cover crops during fallow periods. The objective of increasing carbon input can be also gained by means of the addition of FYM amendments.

In this section, in view of the achievement of neutrality for SOC indicator, we look for the FYM amendments able to reverse a negative departure of SOC change index in arable soils. The theoretical tools are given by Theorem 2 and Corollary 1: the idea is to determine the temporal evolution of the function $f(t)$ or all $t \in]t_0+nT, t_0+(n+1)T]$ and $n = 1, 2, \ldots$, in such a way that the FYM input term $f(t)\mathbf{a}^{(f)}$ assures that the SOC carbon index values $soc(t)$ are above the baseline value $soc(t_0)$ assumed at the initial time. The following result can be derived.

Theorem 7 *The solution* $\Delta soc(t)$ *of* Eq. 14 *corresponding to the solution* $\Delta\mathbf{c}(t)$ *of* Eq. 13 *with normalized farmyard manure rate* $\dfrac{f(t)}{P(t_0)+F(t_0)} = \max\left[0, q_\xi(t)\right]$ *where*

$$q_\xi(t) := \rho(t)\left[\delta\mathbf{k}^{\mathsf{T}}\Delta\mathbf{c}(t) + \frac{1}{T\rho^{(0)}(r)}\right] - \xi N_P^{(n)}\hat{g}_r(t),$$

is positive for all $t \in]t_0+nT, t_0+(n+1)T]$ *and* $n = 1, 2, \ldots$.

Proof Notice that $\frac{d}{dt}\Delta soc(t) = -q_\xi(t) + \max\left[0, q_\xi(t)\right]$. For all $t \in]t_0+nT, t_0+(n+1)T], n = 1, 2, \ldots, \frac{d}{dt}\Delta soc(t) = 0$ if $q_\xi(t) \geq 0$ or $\frac{d}{dt}\Delta soc(t) > 0$ when $q_\xi(t) < 0$. Consequently, $\frac{d}{dt}\Delta soc(t) \geq 0$ and, from $\Delta soc(t_0) = 0$ it follows that $\Delta soc(t) \geq 0$ for all $t \in]t_0+nT, t_0+(n+1)T], n = 1, 2, \ldots$. □

The positive quantity $\max\left[0, q_\xi(t)\right]$ is referred to as *the normalized fertilization rate*, i.e. the rate of fertilization, normalized with respect to the total initial carbon input, which assures positive trends of the SOC change index $\Delta soc(t)$.

For seek of clarity, let us explicitly consider three illustrative cases.

- Case $\xi = 1$. This case corresponds to $F(t_0) = 0$, i.e. a null initial fertilization input. For example, this is the case of arable unfertilized land for which is intended to undertake a farmyard manure amendment that manages to keep positive the trend of SOC. Starting from $\Delta\mathbf{c}(t_0+T) = \mathbf{0}$ we solve

  $$\frac{d\Delta\mathbf{c}}{dt} = \rho(t)A\Delta\mathbf{c} + \left(N_P^{(n)}\hat{g}_r(t) - \frac{\rho(t)}{T\rho^{(0)}(r)}\right)\mathbf{a}^{(g)} + \max\left[0, q_1(t)\right]\mathbf{a}^{(f)},$$

  with

  $$q_1(t) = \rho(t)\left[\delta\mathbf{k}^{\mathsf{T}}\Delta\mathbf{c}(t) + \frac{1}{T\rho^{(0)}(r)}\right] - N_P^{(n)}\hat{g}_r(t),$$

  for all $t \in]t_0+nT, t_0+(n+1)T], n = 1, 2, \ldots$. The specific rate of the farmyard manure amendment necessary to keep SOC change positive can be only evaluated once $P(t_0)$ is known[3] and it is given by

  $$f(t) = \max\left[0, q_1(t)\right]P(t_0).$$

- Case $\xi = 1/2$. This case corresponds to $P(t_0) = F(t_0)$. This means that the fertilization program in the reference year $[t_0, t_0+T]$ has provided an addition of

[3]If the initial distribution of carbon in soil compartments $\mathbf{c}(t_0)$ is known, we can evaluate $P(t_0)$ from Eq. 10.

carbon input equal to the one due to plant residuals. Starting from $\Delta\mathbf{c}(t_0+T)=\mathbf{0}$ we solve

$$\frac{d\Delta\mathbf{c}}{dt} = \rho(t)A\Delta\mathbf{c} + \frac{1}{2}\left(N_P^{(n)}\hat{g}_r(t) - \frac{\rho(t)}{T\rho^{(0)}(r)}\right)\mathbf{a}^{(g)} - \frac{\rho(t)}{2T\rho^{(0)}(r)}\mathbf{a}^{(f)} + \max\left[0, q_{\frac{1}{2}}(t)\right]\mathbf{a}^{(f)},$$

with

$$q_{\frac{1}{2}}(t) = \rho(t)\left[\delta\mathbf{k}^{\mathsf{T}}\Delta\mathbf{c}(t) + \frac{1}{T\rho^{(0)}(r)}\right] - \frac{1}{2}N_P^{(n)}\hat{g}_r(t),$$

for all $t \in]t_0+nT, t_0+(n+1)T], n = 1,2,\ldots$. As before, the specific fertilization rate necessary to keep SOC change positive can be only evaluated once $P(t_0)+F(t_0) = 2P(t_0) = 2F(t_0)$ is known (or evaluated from Eq. 10) and it is given by

$$f(t) = 2\max\left[0, q_{\frac{1}{2}}(t)\right]P(t_0).$$

– Case $\xi = 0$. This case corresponds to $P(t_0) = 0$, i.e. a null initial plant carbon input. For example, a land at rest in the reference year and subjected to a farmyard manure treatment may fall in this case. Starting from $\Delta\mathbf{c}(t_0+T)=\mathbf{0}$ we solve

$$\frac{d\Delta\mathbf{c}}{dt} = \rho(t)A\Delta\mathbf{c} - \frac{\rho(t)}{T\rho^{(0)}(r)}\mathbf{a}^{(f)} + \max\left[0, q_0(t)\right]\mathbf{a}^{(f)},$$

with

$$q_0(t) := \rho(t)\left[\delta\mathbf{k}^{\mathsf{T}}\Delta\mathbf{c}(t) + \frac{1}{T\rho^{(0)}(r)}\right],$$

for all $t \in]t_0+nT, t_0+(n+1)T], n = 1,2,\ldots$. When $F(t_0)$ is available (or evaluated by Eq. 10) we can deduce the specific fertilization rate $f(t)$ from its normalized quantity:

$$f(t) = \max\left[0, q_0(t)\right]F(t_0).$$

In Section 8.2.2 we will illustrate the distribution of the normalized fertilization rate $\max\left[0, q_\xi(t)\right]$ for $\xi = 1,\ 1/2, 0$ in the case when the model is applied to a protected zone in the Italian Apulian region, with environmental and weather conditions in the years 2006-2019.

7 A non-standard approximation of SOC changes

In [20] the author proved that the original discrete RothC model in [3] can be thought of as a one-step, first-order in time, discretization of the continuous model (1). In light of this interpretation, a novel non-standard first-order approximation, which inherits the discrete decomposition process of the original model and has the same equilibrium state of the continuous dynamics (1), was proposed in [5]. When applied as a monthly time-stepping procedure, it can be considered a suitable alternative to the original discrete RothC model. In monthly units the annual length corresponds to $T=12$ and the interval $[t_0+nT, t_0+(n+1)T]$ is discretized in the set of instants $t_m^{(n)} := t_{m-1}^{(n)} + \Delta t_m$, with $m = 1,\ldots,12$ and $t_0^{(n)} := t_0 + nT$. The step lengths are set as $\Delta t_m := \dfrac{T}{365}N_m \approx 1$, where N_m is the number of days of the mth month of the nth year. By denoting with I the 4-dimensional identity matrix, and setting $\mathbf{f}(\mathbf{c};t) := \rho(t)A\mathbf{c} + \mathbf{b}(t)$ and $\widetilde{A} := -(I-\Lambda)D(I-\Lambda)^{-1}$, with

$$\Lambda = \begin{pmatrix} 0 & 0 & 0 & 0 \\ 0 & 0 & 0 & 0 \\ \alpha & \alpha & \alpha & \alpha \\ \beta & \beta & \beta & \beta \end{pmatrix}, \quad D = \begin{pmatrix} k_{dpm} & 0 & 0 & 0 \\ 0 & k_{rpm} & 0 & 0 \\ 0 & 0 & k_{bio} & 0 \\ 0 & 0 & 0 & k_{hum} \end{pmatrix},$$

the approximated values $\mathbf{c}_m^{(n)} \approx \mathbf{c}(t_m^{(n)})$ of the solution of Eq. 12, are given by

$$\mathbf{c}_{m+1}^{(n)} = \mathbf{c}_m^{(n)} + \Delta t_m \varphi(\Delta t_m \rho(t_m^{(n)})\widetilde{A})\mathbf{f}(\mathbf{c}_m^{(n)}; t_m^{(n)}) \tag{24}$$

or, equivalently,

$$\mathbf{c}_{m+1}^{(n)} = F(\Delta t_m \rho(t_m^{(n)}))\mathbf{c}_m^{(n)} + \Delta t_m \varphi(\Delta t_m \rho(t_m^{(n)})\widetilde{A})\mathbf{b}(t_m^{(n)}), \tag{25}$$

where $F(t) := \Lambda + (I-\Lambda)e^{-tD}$ and $\Delta t_m \varphi(\Delta t_m \rho(t_m^{(n)})\widetilde{A}) = \mathcal{O}(diag(\Delta t_m))$ [5], the function φ being defined in Eq. 20. The formulation (24) emphasizes the sharing of the stationary equilibria of the continuous autonomous model $\dfrac{d\mathbf{c}}{dt} = \mathbf{f}(\mathbf{c})$ in case when the explicit temporal dependence is neglected and temporal averaged quantities are exploited. Formulation (25) highlights the similarity with the discrete original RothC model which proceeds according to

$$\mathbf{c}_{m+1}^{(n)} = F(\Delta t_m \rho(t_m^{(n)}))\mathbf{c}_m^{(n)} + \Delta t_m \mathbf{b}(t_m^{(n)}). \tag{26}$$

In this paper, we are interested in finding an analogous monthly time-stepping procedure for approximating the changes of $\mathbf{c}(t)$ provided by the evolution of the variable $\Delta\mathbf{c}(t)$. From the observation that the homogeneous systems for $\mathbf{c}(t)$ and $\Delta\mathbf{c}(t)$ are both governed by the matrix $\rho(t)A$, it makes sense to use the non standard procedure described above. Consequently, the approximated values $\Delta\mathbf{c}_m^{(n)} \approx \Delta\mathbf{c}(t_m^{(n)})$ of the solution of Eq. 13, are given by

$$\Delta\mathbf{c}_{m+1}^{(n)} = \Delta\mathbf{c}_m^{(n)} + \Delta t_m \varphi(\Delta t_m \rho(t_m^{(n)})\widetilde{A})\mathbf{f}(\Delta\mathbf{c}_m^{(n)}; t_m^{(n)}) \tag{27}$$

or, equivalently,

$$\Delta\mathbf{c}_{m+1}^{(n)} = F(\Delta t_m \rho(t_m^{(n)}))\Delta\mathbf{c}_m^{(n)} + \Delta t_m \varphi(\Delta t_m \rho(t_m^{(n)})\widetilde{A})\mathbf{b}(t_m^{(n)}), \tag{28}$$

where, with abuse of notation, $\mathbf{f}(\Delta\mathbf{c};t) = \rho(t)A\Delta\mathbf{c} + \mathbf{b}(t)$ and

$$\mathbf{b}(t) = \left(N_P^{(n)}\hat{g}_r(t) - \frac{\rho(t)}{T\rho^{(0)}(r)}\right)\mathbf{a}^{(g)}$$

in case of no farmyard manure input, while

$$\mathbf{b}(t) = \left(N_P^{(n)}\hat{g}_r(t) - \frac{\rho(t)}{T\rho^{(0)}(r)}\right)\xi\mathbf{a}^{(g)} - \frac{\rho(t)}{T\rho^{(0)}(r)}(1-\xi)\mathbf{a}^{(f)} + \frac{f(t)}{P(t_0)+F(t_0)}\mathbf{a}^{(f)},$$

where $0 < \xi := \dfrac{P(t_0)}{P(t_0)+F(t_0)} < 1$, in the opposite case.

Finally, $\Delta soc(t_m^{(n)})$ are approximated by $\Delta soc_m^{(n)} := \mathbb{1}^\intercal \Delta \mathbf{c}_m^{(n)}$, for $m = 1, \ldots, 12$ and $n = 1, 2 \ldots$.

8 A test case: trends of *SOC* changes in the Alta Murgia National Park

As an application of the illustrated procedure, we analyze the change of SOC in the Alta Murgia National Park, a protected area in the Italian Apulia region, southern Italy, established in 2004 (see Fig. 3). Two parameters are fixed for all the land surface area of 68077 ha, i.e. the depth layer is fixed at $d = 23$ cm and the clay content is set at the percentage $cly = 50$, i.e. the value used in [7] for experiments at the experimental farm of the CRA-Cereal Research Centre (41 °C 27′ N, 15 °C 30′ E) in Foggia. Temperature, rainfull, diurnal temperature range from 2005 to 2019 at (40 °C 75′ N, 16 °C 75′ E,) are extracted from the CRU TS 4.04 grid-box dataset [11] of the Climatic Research Unit (University of East Anglia) and NCAS (see Fig. 4). Potential evapotranspiration is calculated from the available climate data according to the Thornthwaite's formula given in the Appendix. Estimates of the Net Primary Production across Earth's entire vegetated land surface are taken from the MOD17 project,[4] part of the NASA Earth Observation System (EOS) program, which is the first satellite-driven dataset [23] to monitor vegetation productivity on a global scale. We have extracted the NPP data in the temporal range from 2005 to 2019 by means of the Application for Extracting and Exploring Analysis Ready Samples (AppEEARS) [26] in a polygonal containing the boundary of the Alta Murgia Park (see Fig. 5).

In Fig. 6 we report the annual NPP values and the averaged annual temperatures with respect to their reference values set at $t_0 = 2005$, extracted by the above dataset. As expected, to increasing temperatures correspond increasing values for NPP.

Three different formulations are used for modelling the periodic function $\hat{g}_r(t)$. For values of $r \in r(a) := \{r \geq 1\}$ corresponding to the arable class, we set $\hat{g}_r(t) = \hat{g}_{r(a)}(t)$; for $r \in r(g) := \{0.5 \leq r < 1\}$ associated with the grassland class, $\hat{g}_r(t) = \hat{g}_{r(g)}(t)$ and we set $\hat{g}_r = \hat{g}_{r(f)}(t)$ in correspondence of the forest class described by values $r \in r(f) := \{0 \leq r \leq 0.5\}$. The monthly values at $t = t_m^{(n)}$ for $m = 1, \ldots 12$, of the three main land use distributions $\hat{g}_{r(a)}, \hat{g}_{r(g)}, \hat{g}_{r(f)}$ are reported in Table 1. The reported values are assumed equal to the distribution of plant carbon inputs given in [9] which mimics the dynamics of typical crop rotations and permanent grassland or forest in Europe. Finally, in Table 1 we report also the values for $k_c(t, r)$ at $t = t_m^{(n)}$, for the three main land use, i.e $k_c(t_m^{(n)}, r(a)), k_c(t_m^{(n)}, r(g)), k_c(t_m^{(n)}, r(f))$, assuming that the soil cover function $S_r(t)$ is periodic. Plant cover was assumed to occur in months 1–7 and 12 for the arable (croplands) class [25].

8.1 Numerical trends of sensitivity from 2005 to 2007

In this section, using the Alta Murgia National Park data in the period 2005–2007 we want to show the behaviour of the sensitivities of the SOC change index to average annual temperature, to the relative value of NPP and to $r =$ DPM/RPM ratio. We chose $t_0 = 2005T$, with $T = 12$, thus $Temp^{(1)} = 14.27$ °C is the average temperature of 2006 and $N_P^{(1)} = 1.08$ is the ratio between the Net Primary Production of 2006 and the Net Primary Production of 2005. Once we have computed the numerical solution of the Cauchy problem (17), we obtain the sensitivities by summing up the four components of the numerical solution of the initial value problems Eqs. 29, 30 and 31 (see Appendix).

The numerical approximation of the sensitivity to the average temperature in 2006, depicted in Fig. 7a, is a negative function of time, consistently with Theorem 4. Thus, an increase in the average temperature of 2006 would have reduced Δsoc during the year and, consequently, the sum of the soil carbon contained in compartments would have decreased too.

Moreover, since the sensitivity of Δsoc to $Temp^{(1)}$ is a decreasing function of time, we can deduce that the perturbation in the average temperature of 2006 would have affected the rate of decomposition at every month, and this effect would have been amplified over time.

Analogously, we can observe that the numerical approximation of the sensitivity of Δsoc to $N_P^{(1)}$ is consistent with Theorem 5. In fact, in Fig. 7b it is depicted as a positive (and increasing) function of time. This means that an increase in the Net Primary Production in 2006 with respect to the Net Primary Production in 2005, would have increased Δsoc, and consequently the sum of the soil carbon contained in compartments, during the year. Moreover, the perturbation in $N_P^{(1)}$ would have affected the rate of decomposition at every month with this effect amplified over time although at a decreasing pace.

[4]https://www.ntsg.umt.edu/project/modis/mod17.php

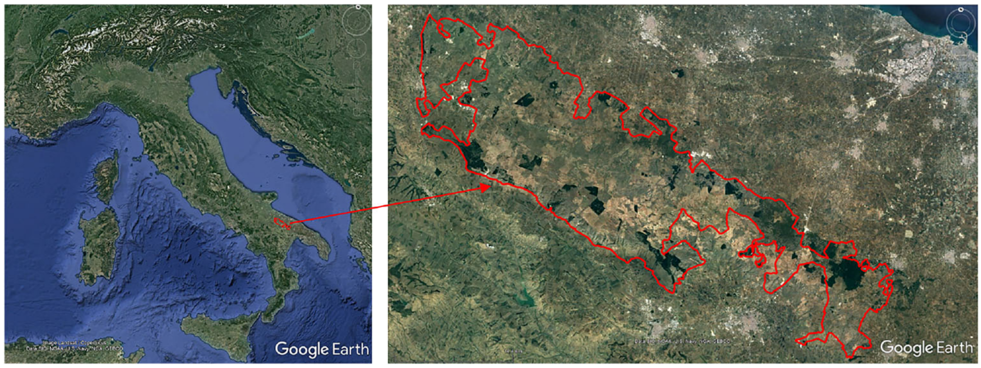

Fig. 3 Boundaries of the Alta Murgia National Park from Google Earth

Finally, let us focus on the sensitivity of Δsoc to the parameter r. According to our data, $\vartheta^{(1)} = 4.3620 \cdot 10^{-4}$. Thus, since $\vartheta^{(1)}$ is positive, by Theorem 6 we have that the sensitivity is a negative function of time and this is consistent with Fig. 7c. Thus, an increase in the parameter r at the beginning of 2006, i.e. a transition from forest to grassland and to arable classes, would have caused a decrease in Δsoc and the sum of the soil carbon over the compartments during that year. Also in this case, the perturbation in r would have affected the rate of decomposition at every month, again with an amplification of the effect over time.

8.2 SOC changes scenarios in years 2005–2019

We are going to illustrate the evolution of SOC changes in the Alta Murgia National Park in the period 2005–2019 taking as the baseline its distribution in 2005 ($t_0 = 2005T$ with $T = 12$). The approximated values $\Delta \mathbf{c}_m^{(n)} \approx \Delta \mathbf{c}(t_m^{(n)})$ of the solution of Eq. 13 for $t_m^{(n)} \in [t_0 + nT, t_0 + (n+1)T]$ with $n = 1, \ldots, 14$, provided by means of the non-standard discrete procedure described in Eq. 28, are evaluated for the three main land use classes: forest, grassland and arable. For the arable case, we also show the farmyard manure program which would be able to assure the achievement of land degradation neutrality in 2019 with respect to 2005 taken as the reference year.

8.2.1 SOC changes in forest and grassland classes

For the forest and grassland classes, the evolution of $\Delta soc(t_m^{(n)})$, together with its averaged annual values, is given in Figs. 8 and 9, respectively. For the forest class, we set $r = 1e-4$, $r = 0.25$ (i.e. the value used in the case of forest class in literature [3]), and $r = 0.5$ in order to span all the values corresponding to this class. We notice that, for r spanning the reference set $r(f)$, the trends do not differ much. For the grassland class, we set $r = 0.67$ (i.e. the value used in the case of grassland class in literature [3]), $r = 0.9$ and $r = 0.95$ in order to span all the values corresponding to this class. Notice that, differently from the forest scenario, the dynamics of the SOC change index are much influenced by the value of r. For both land use classes the general trend of Δsoc, even oscillating, is towards decreasing values. This suggests a scenario of loss of soil carbon stocks for both land use classes.

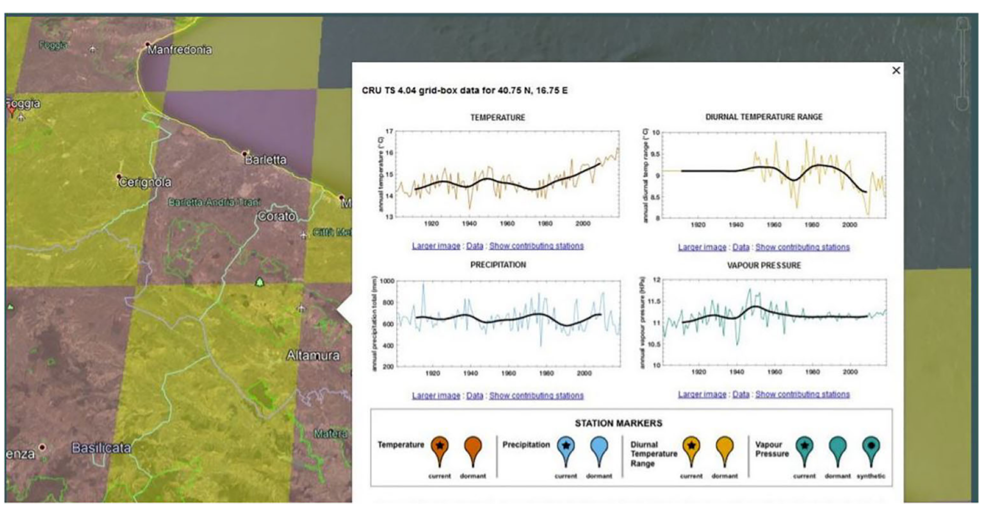

Fig. 4 Climate data at (40 °C 75′ N, 16 °C 75′ E) from CRU TS 4.04 grid-box dataset of the Climatic Research Unit (University of East Anglia)

Fig. 5 Selected layer and temporal values of NPP from the MOD17 project of the NASA EOS program

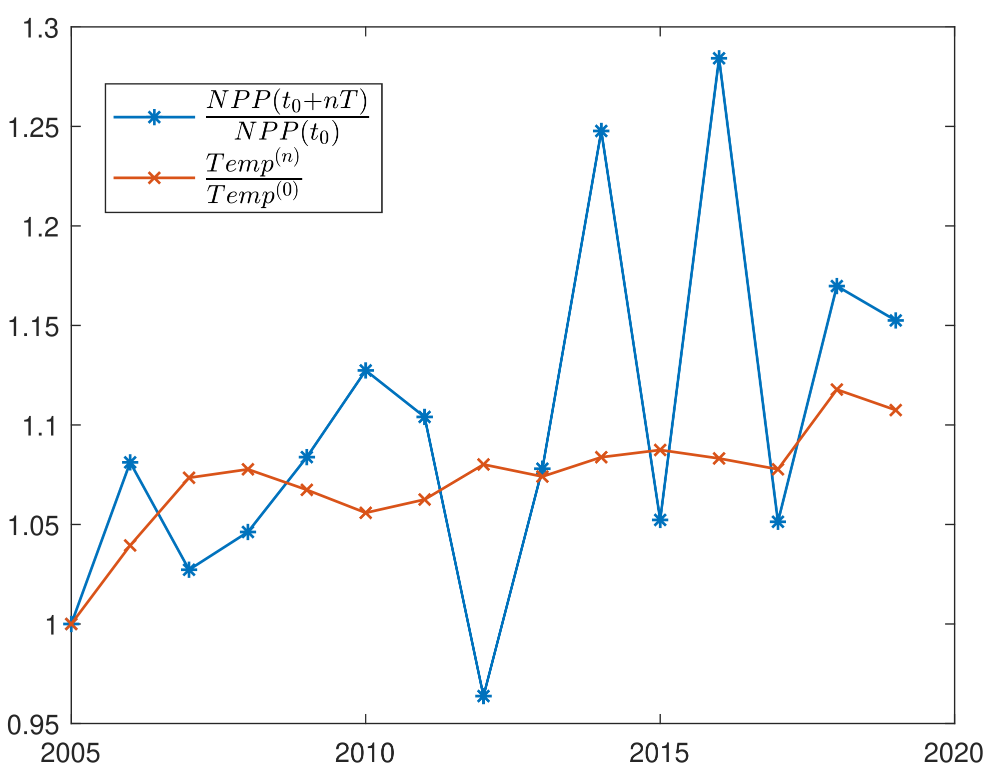

Fig. 6 Behaviour of relative values of NPP and annual averaged temperatures in temporal interval [2005, 2019] with respect to their initial values

Table 1 Monthly ($t = t_m^{(n)}$, n = 0, 1, 2, ...) distribution of plant carbon inputs into the soil expressed as a proportion of the total $\hat{g}_r(t)$ and rate modifying factor $k_c(t, r)$ related to soil cover. Data from [9] and [25]

t	$\hat{g}_{r(a)}(t)$	$k_c(t, r(a))$	$\hat{g}_{r(g)}(t)$	$k_c(t, r(g))$	$\hat{g}_{r(f)}(t)$	$k_c(t, r(f))$
$t_1^{(n)}$ (Jan, 31)	0.0	0.6	0.05	0.6	0.025	0.6
$t_2^{(n)}$ (Febr, 28)	0.0	0.6	0.05	0.6	0.025	0.6
$t_3^{(n)}$ (Mar, 31)	0.0	0.6	0.05	0.6	0.025	0.6
$t_4^{(n)}$ (Apr, 30)	1/6	0.6	0.05	0.6	0.025	0.6
$t_5^{(n)}$ (May, 31)	1/6	0.6	0.10	0.6	0.05	0.6
$t_6^{(n)}$ (Jun, 30)	1/6	0.6	0.15	0.6	0.05	0.6
$t_7^{(n)}$ (Jul, 31)	0.5	0.6	0.15	0.6	0.05	0.6
$t_8^{(n)}$ (Aug, 31)	0.0	1	0.10	0.6	0.05	0.6
$t_9^{(n)}$ (Sept, 30)	0.0	1	0.10	0.6	0.20	0.6
$t_{10}^{(n)}$ (Oct, 31)	0.0	1	0.10	0.6	0.20	0.6
$t_{11}^{(n)}$ (Nov, 30)	0.0	1	0.05	0.6	0.20	0.6
$t_{12}^{(n)}$ (Dec, 31)	0.0	0.6	0.05	0.6	0.10	0.6

8.2.2 SOC change in arable class and fertilization program

For the arable class, we firstly assume that no farmyard manure enters the system so that the evolution of $\Delta soc(t_m^{(n)})$, together with its averaged annual values, is given in Fig. 10. We set $r = 1$, $r = 1.44$ (i.e. the value used in the case of forest class in literature [3]), and $r = 100$ in order to span all the values corresponding to this class. This case is the most critical one: the general trend departing from the baseline of positive values is much more pronounced.

An indirect proof of this trend can be extrapolated by an experiment run in the area whose environmental conditions and soil composition have been used for the model parameter settings. The experiment was performed

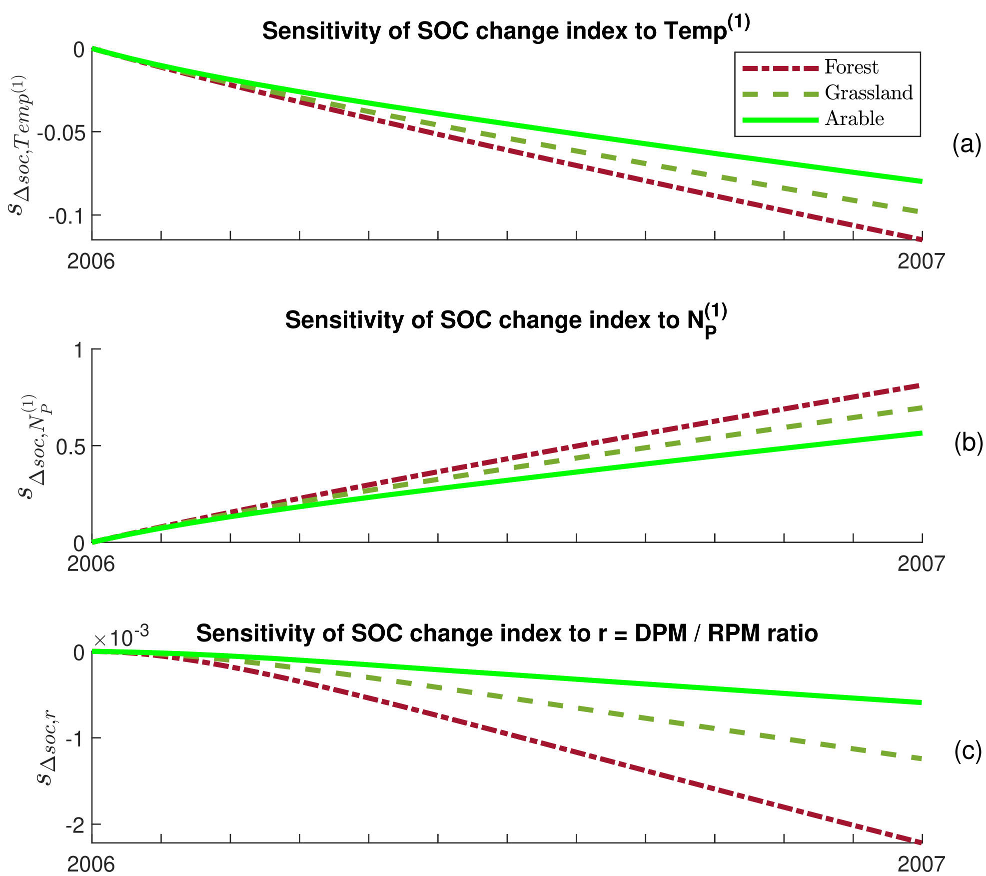

Fig. 7 Numerical non-standard approximation of the temporal evolution of $s_{\Delta soc, Temp^{(1)}}$, $s_{\Delta soc, N_P^{(1)}}$ and $s_{\Delta soc, r}$ in 2006, with time-step $\Delta t = 0.01$. Parameters: $r = 0.25$ for the forest class, $r = 0.67$ for the grassland class and $r = 1.44$ for the arable class

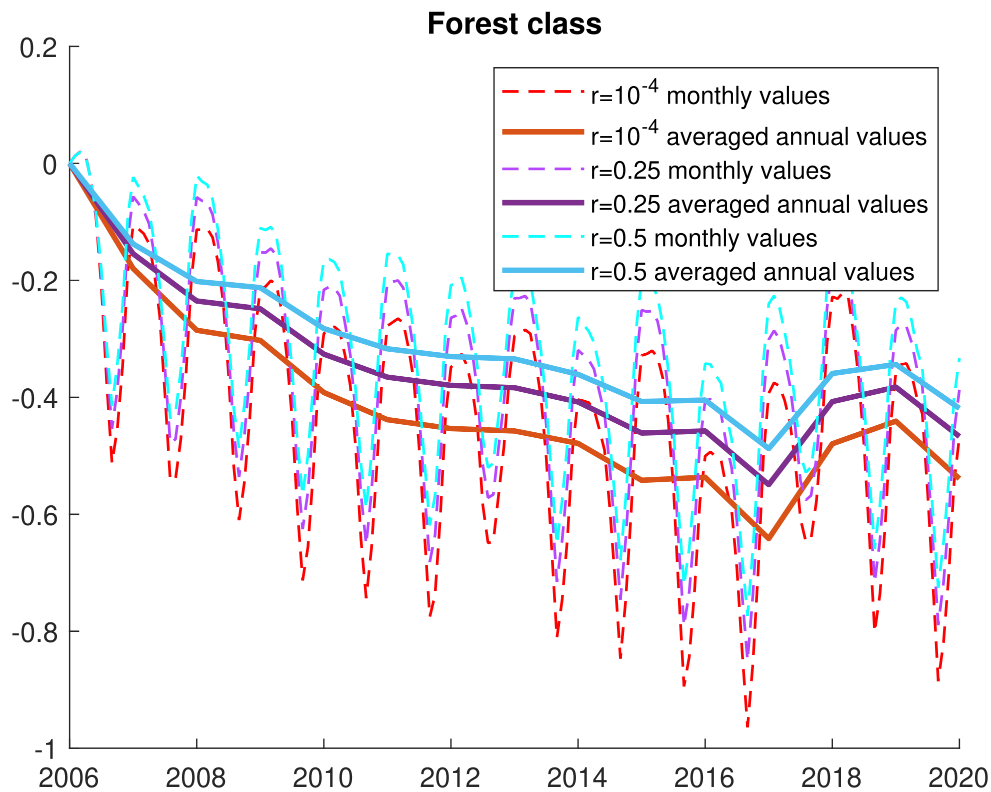

Fig. 8 The temporal evolution of $\Delta soc(t_m^{(n)})$, together with its averaged annual values (arithmetic annual means of the monthly simulated values) for the forest class. Parameters $r = 10^{-4}$, $r = 0.25$, $r = 0.5$

on a time span of 16 years, partially overlapping with the time interval considered in our study [1]. A similar trend in temperature and NPP has been observed for both the experiment and our analysis. The result of the experiment is an overall 14% decrease of SOC thus confirming, at least qualitatively, the results shown in Fig. 10.

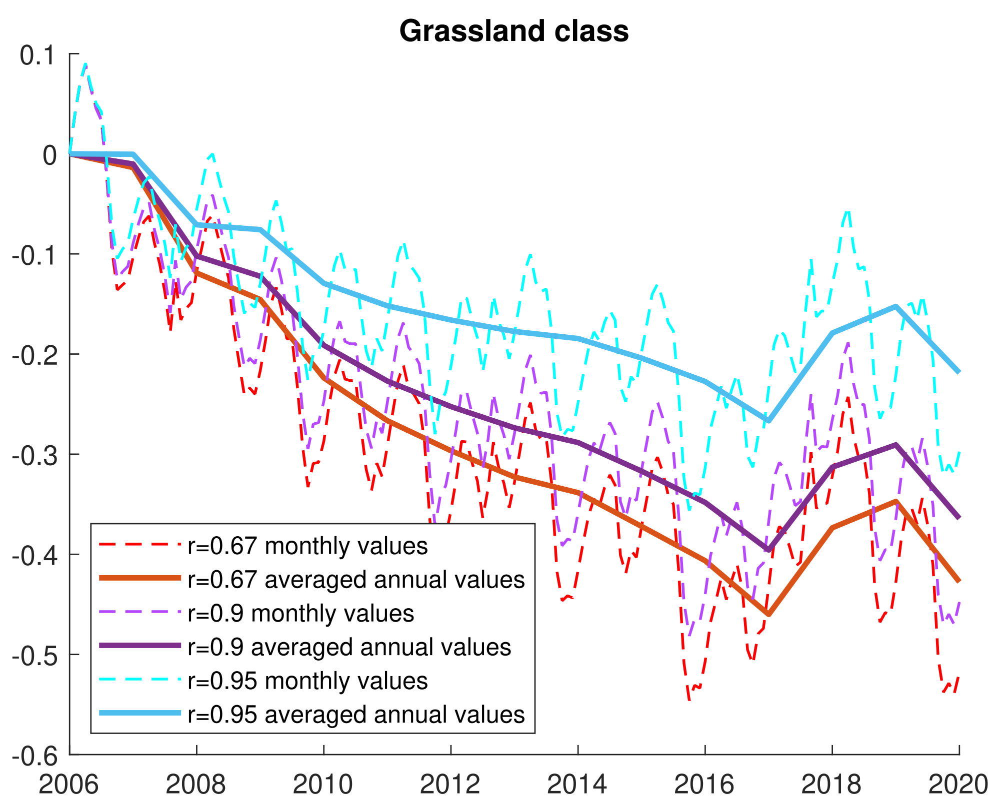

Fig. 9 The temporal evolution of $\Delta soc(t_m^{(n)})$, together with its averaged annual values (arithmetic annual means of the monthly simulated values) for the grassland class. Parameters $r = 0.67$, $r = 0.9$, $r = 0.95$

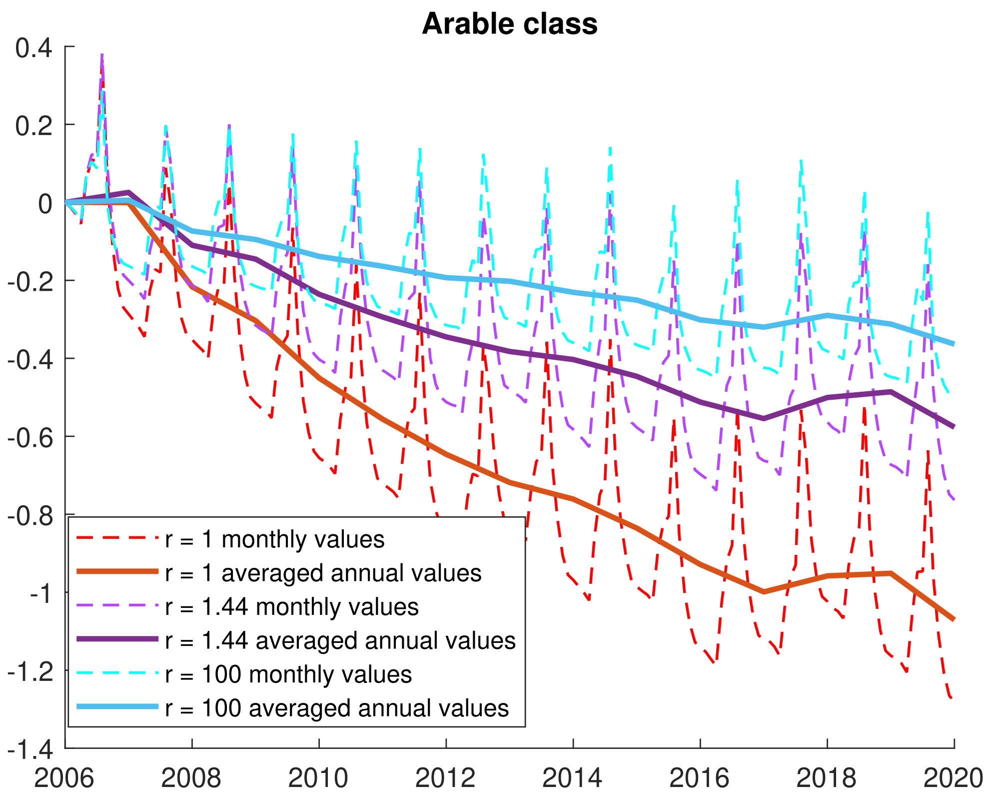

Fig. 10 The temporal evolution of $\Delta soc(t_m^{(n)})$, together with its averaged annual values (arithmetic annual means of the monthly simulated values) for the arable class. Parameters $r = 1$, $r = 1.44$, $r = 100$

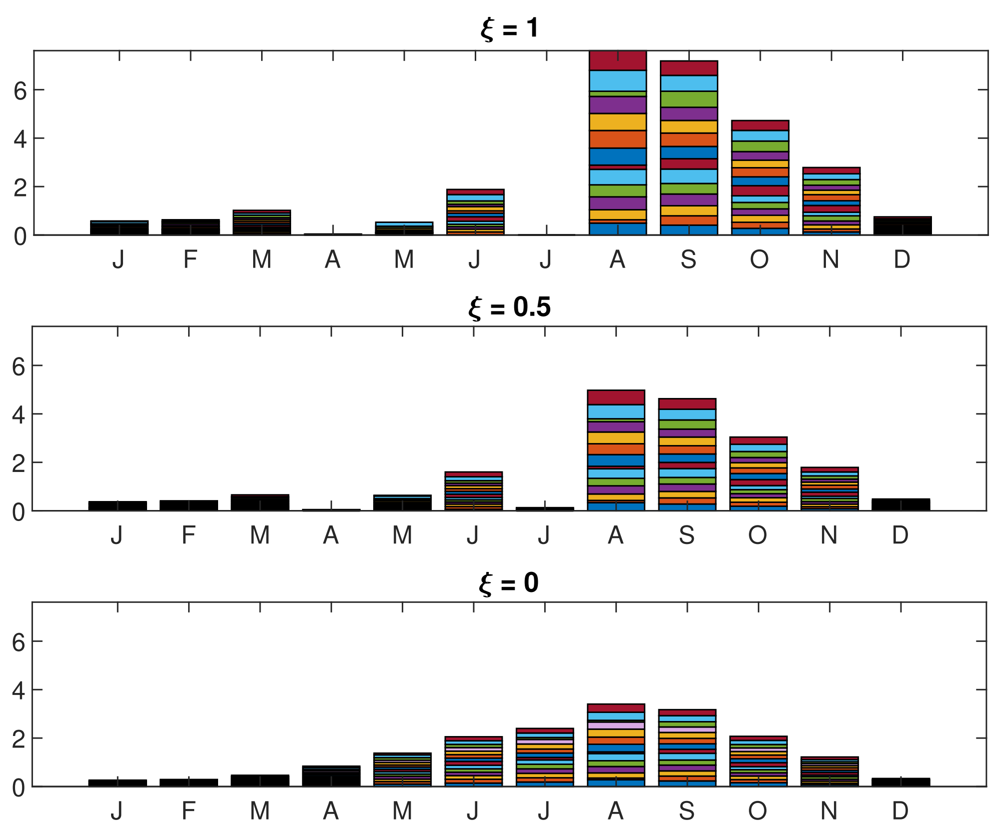

Fig. 11 Box plot (with stacked values of 14 consecutive years) of the normalized fertilization rate $\max\left[0, q_{\xi}(t)\right]$ for the arable class with $r = 1.44$. Parameter $\xi = 1$ (only plant initial carbon input i.e. $F(t_0) = 0$), $\xi = 0.5$ (same content of plant and FYM initial carbon inputs i.e. $P(t_0) = F(t_0)$), $\xi = 0$ (only FYM initial carbon input i.e. $P(t_0) = 0$)

For this class, in order to reach positive quantities, it is necessary to intensify the organic carbon input. To this aim, we can apply the findings of Theorem 7 in order to detect the farmyard manure program necessary to enforce positive values of Δsoc. In Fig. 11 we report the monthly boxes of the *normalized fertilization rate* $\max\left[0, q_\xi(t)\right]$, stacked on the years 2006–2019 for the arable class as defined in Theorem 7, for values of $\xi = 1, 1/2, 0$. From the stacked plot we see that the normalized fertilization rate increases with ξ and during the years, is distributed with a maximum value around August and decreases from August to December. Low values are generally taken on winter months but the lowest rates are assumed in April and July for values of $\xi > 0$ corresponding to an initial non null carbon input coming from plant residual ($P(t_0) \neq 0$). The effects of the fertilization process are shown in Fig. 12 in which we have added the case corresponding to $\xi = 0.8$. The greatest effect in increasing the SOC change index due to the farmyard amendments is obtained in correspondence of $\xi = 1$, which is the case when the initial carbon input is only due to the plant residual and no fertilization program has been implemented in the reference year ($F(t_0) = 0$). On the contrary, the lowest effect of the fertilization action provides a constant (null) SOC index for $\xi = 0$. This is the case of $P(t_0) = 0$ which corresponds, for example, to land at rest where farmyard manure has been applied. In this case, no initial contribution to carbon input is supposed to come from plant residuals.

9 Comments and future research directions

Soil carbon models (e.g. RothC [3], Century [22]), which take into account the interactions between climate and land use management, are widely used to predict SOC changes under future climate scenarios. Warmer temperatures positively affect SOC stocks since they reduce decomposition, as an effect of decreased soil moisture, and also increase Net Primary Production thus augmenting carbon inputs to the soil. On the other hand, increasing temperatures negatively affect SOC stocks as they increase the decomposition rate of soil organic matter. Hence, whether soils gain or lose SOC depends upon how balanced the competing gain and loss processes are, with subtle interacting changes in temperature, moisture, soil type and land use [9].

With the aim of improving the prediction of the factors that determine the size and direction of change, we have introduced the so-called *SOC change index* and we have described its evolution based on the RothC carbon model. Under the hypothesis of constant environmental and organic fertilization conditions, it does not require evaluating or measuring the specific initial value of SOC, as it describes the deviation from the assumed initial equilibrium.

Fig. 12 The temporal evolution of $\Delta soc(t)$, together with its averaged annual values for the arable class with $r = 1.44$ controlled by farmyard manure. Increasing values of $\Delta soc(t)$ for parameters $\xi = 0$ (only FYM initial carbon input) , $\xi = 0.5, 0.8$, and $\xi = 1$ (only plant initial carbon input)

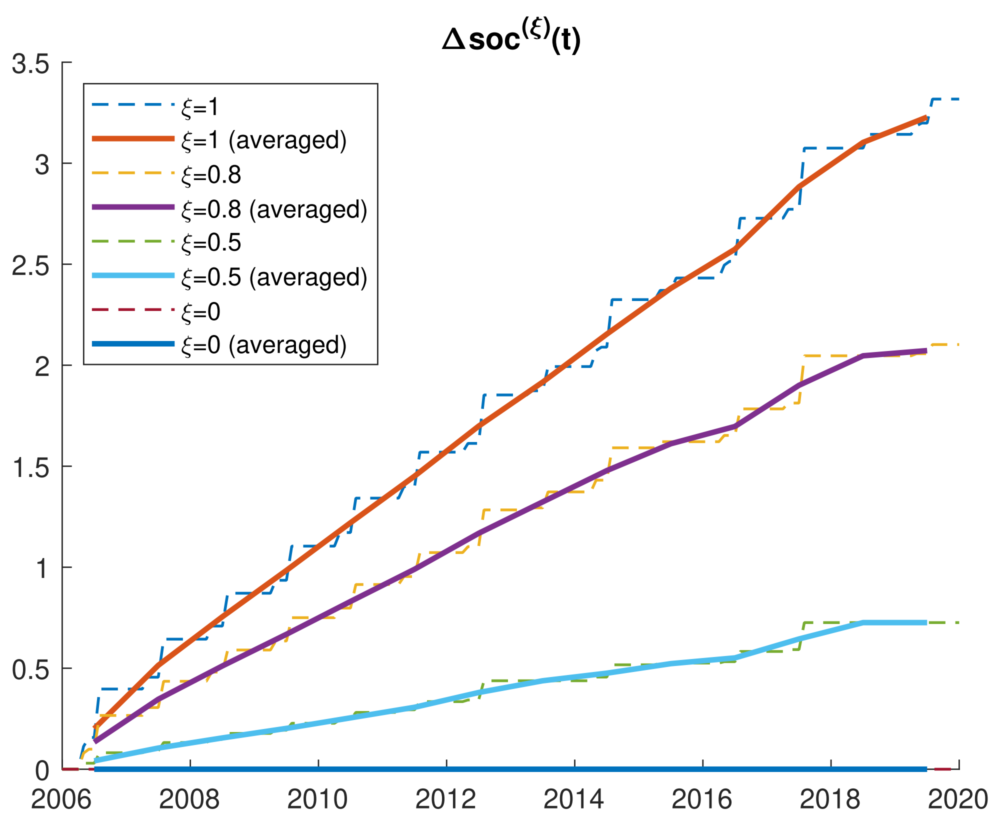

The strength of our method is in the context of a land degradation analysis [18]. Indeed, for establishing if land degradation neutrality (LDN) has been achieved or not, we need only to establish the sign of the change of the main indicators with respect to an initial value taken as a baseline.

As concern the SOC indicator to establish the sign of its change, in absence of farmyard manure inputs, by means of the classical RothC method, one needs

1. available measured data about the initial total carbon content $soc(t_0)$ and its distribution among the pools $\mathbf{c}(t_0)$;
2. to run the model in 'reverse' mode to establish the initial plant carbon input $P(t_0)$ which makes $\mathbf{c}(t_0)$ the initial equilibrium state of the system;
3. to run the model in forward mode to evaluate $soc(t)$;
4. to perform the difference $soc(t) - soc(t_0)$ to establish the sign of the change.

To make the same prevision with the proposed methodology, one only needs to run the model for the variable $\Delta\mathbf{c}$ starting from the null initial value and check the sign of the sum of its components which provides the value of $\Delta soc(t)$. Indeed, the dynamics of $\Delta\mathbf{c}$ given in Eq. 16 do not depend on $P(t_0)$ nor on $\mathbf{c}(t_0)$ and $\Delta soc(t)$ has the same sign of the SOC change since $\Delta soc(t) := \dfrac{soc(t) - soc(t_0)}{P(t_0)}$ with $P(t_0) > 0$.

The simulation example here proposed presents the kind of qualitative results that our model is able to provide. The effectiveness of the SOC change index has been tested for evaluating the impact of warming temperatures on the achievement of land degradation neutrality for the SOC indicator in Alta Murgia National Park, a protected area in the Apulia region located in the south of Italy. The performed sensitivity analysis, based on time-averaged parameter values, has provided local information on the impact of change in mean annual temperature, of deviations of the mean annual NPP from its reference value and of the degree of decomposability of plant material. The results of the sensitivity analysis are in accordance with the experimental results, as we found that the SOC change index is negatively affected by increasing mean annual temperature and positively by increasing deviation of NPP. Changes in DPM/RPM ratio r, which in turn are related to land use change, indicate that all land use classes are positively affected when the deviation of NPP prevails on deviation in decomposition and negatively in the opposite case. In both cases, the arable class is the most affected.

The simulated dynamics of the SOC change index in the Alta Murgia National Park in years [2005, 2019] with climate data of CRU (University of East Anglia) and estimates of NPP taken from the MOD17 project indicate negative trends for all the land use classes. The arable class, which is most affected by changes in NPP and temperature, as suggested by our sensitivity analysis, shows a more pronounced negative trend, which is supported by some in-field experiments.

In view of the achievement of neutrality for SOC indicator, we have determined the *normalized fertilization rate* able to reverse a negative departure of the SOC change index in arable soils. The dynamics of the SOC change index under the hypothesis of farmyard manure input has revealed a powerful tool for predicting the suitable land fertilization practice to implement for enhancing the SOC stocks in the arable soil of Alta Murgia Park and invert the negative trend.

In this paper, the dynamics of the SOC change index has been tailored to the RothC model. In principle, its dynamics can be described by any soil organic carbon model. The versatility of RothC relies on its special linear functional form which allows to derive in a (almost) 'straightforward' way the specific equations for the SOC change index dynamics. However, we stress that our approach might be generalized to other soil models (for example Century model [22]) along the path here described: tracing the SOC change index under the hypothesis of initial equilibrium and studying its sensitivity to the main parameters. In particular, a future research direction is represented by the description of the SOC change index under a suitable carbon model dynamics which places the action of bacteria at the heart of the mechanisms of the decomposition process as indicated in [10, 13].

The sensitivity analysis identifies the sensitive carbon compartments only in view of their contribution, positive or negative, to the sensitivity of the global SOC metric. To take some general conclusions or to make some meaningful previsions, the qualitative trends of the SOC change index and the qualitative results of its sensitivity analysis to the main parameters should result independent of the soil organic carbon model considered (and the number and the nature of its compartments). This question also deserves to be addressed in the next future.

Appendix

A.1 Proof of Theorem 2

By plugging the expression of $P(t_0 + nT)$ into the Eq. 12, for all $t \in [t_0 + nT, t_0 + (n+1)T]$, and $n = 1, 2, \ldots$, we have

$$\frac{d\mathbf{c}}{dt} = \rho(t)A\mathbf{c} + P(t_0)N_P^{(n)}\hat{g}_r(t)\mathbf{a}^{(g)} + f(t)\mathbf{a}^{(f)}.$$

Thus,

$$\begin{aligned}\frac{d\Delta\mathbf{c}}{dt} &= \frac{1}{P(t_0)+F(t_0)}\left(\rho(t)A\mathbf{c}+P(t_0)N_P^{(n)}\hat{g}_r(t)\mathbf{a}^{(g)}\right.\\ &\quad\left.+f(t)\mathbf{a}^{(f)}\right)\\ &= \rho(t)A\Delta\mathbf{c}+\frac{1}{P(t_0)+F(t_0)}\\ &\quad\left(\rho(t)A\mathbf{c}(t_0)+P(t_0)N_P^{(n)}\hat{g}_r(t)\mathbf{a}^{(g)}+f(t)\mathbf{a}^{(f)}\right)\\ &= \rho(t)A\Delta\mathbf{c}+\frac{P(t_0)}{P(t_0)+F(t_0)}N_P^{(n)}\hat{g}_r(t)\mathbf{a}^{(g)}\\ &\quad+\frac{\rho(t)A\mathbf{c}(t_0)}{P(t_0)+F(t_0)}+\frac{f(t)}{P(t_0)+F(t_0)}\mathbf{a}^{(f)}.\end{aligned}$$

Recalling the relation between $P(t_0)$ and $\mathbf{c}(t_0)$ in Eq. 9 that yields

$$A\mathbf{c}(t_0) = -\frac{1}{T\rho^{(0)}(r)}\left(P(t_0)\mathbf{a}^{(g)}+F(t_0)\mathbf{a}^{(f)}\right),$$

we have

$$\begin{aligned}\frac{d\Delta\mathbf{c}}{dt} &= \rho(t)A\Delta\mathbf{c}+\left(N_P^{(n)}\hat{g}_r(t)-\frac{\rho(t)}{T\rho^{(0)}(r)}\right)\xi\mathbf{a}^{(g)}\\ &\quad-\frac{\rho(t)}{T\rho^{(0)}(r)}(1-\xi)\mathbf{a}^{(f)}+\frac{f(t)}{P(t_0)+F(t_0)}\mathbf{a}^{(f)}.\end{aligned}$$

A.2 Proof of Theorem 3

From

$$\begin{aligned}\frac{d\Delta\mathbf{c}(t_0+T)}{dt} &= \rho(t_0+T)A\Delta\mathbf{c}(t_0+T)\\ &\quad+\vartheta(t_0+T)\mathbf{a}^{(g)} = \vartheta(t_0+T)\mathbf{a}^{(g)}\end{aligned}$$

it results that, for $t = t_0+T+\epsilon$,

$$\Delta\mathbf{c}(t) = \epsilon\vartheta(t_0+T)\mathbf{a}^{(g)}+\mathbf{O}(\epsilon^2);$$

consequently,

$$\Delta\bar{\mathbf{c}}(t)-\Delta\mathbf{c}(t) = \epsilon\left(\vartheta^{(1)}\varphi\left(B(\epsilon)\right)-\vartheta(t_0+T)I\right)\mathbf{a}^{(g)}+\mathbf{O}(\epsilon^2).$$

Notice that the eigenvalues of A, are negative and distinct from each other ($\lambda_1 < \lambda_2 < \lambda_3 < \lambda_4 < 0$), therefore there is a nonsingular matrix $V \in \mathbb{R}^{4\times4}$ such that $A = V^{-1}EV$, where E is the diagonal matrix whose diagonal components are the eigenvalues of A. Consequently, $\varphi(B(\varepsilon))$ is diagonalizable and its eigenvalues are positive and less than one. In fact,

$$\varphi(B(\varepsilon)) = \varphi(\varepsilon\rho^{(1)}(r)A) = V^{-1}\varphi\left(\varepsilon\rho^{(1)}(r)E\right)V,$$

where $\varphi\left(\varepsilon\rho^{(1)}(r)E\right)$ is diagonal and its components are $0 < \varphi(\varepsilon\rho^{(1)}(r)\lambda_i) < 1$, for $i = 1,\ldots,4$ because $\varepsilon\rho^{(1)}(r)\lambda_i < 0$.

Now, let us consider the norm on $\mathbb{R}^4$ such that for all vector $\mathbf{x}\in\mathbb{R}^4$, $\|\mathbf{x}\| := \|V\mathbf{x}\|_2$ and the corresponding matrix norm that for all $M\in\mathbb{R}^{4\times4}$, $\|M\| = \|VMV^{-1}\|_2$. We have that

$$\begin{aligned}\|\varphi(B(\varepsilon))\| &= \|V\varphi(B(\varepsilon))V^{-1}\|_2 = \|\varphi(\varepsilon\rho E)\|_2\\ &= \varphi(\varepsilon\rho^{(1)}(r)\lambda_4) < 1.\end{aligned}$$

Moreover, since all norms on finite-dimensional vector spaces are equivalent, there exists a constant $c > 0$ such that for all vector $\mathbf{x}\in\mathbb{R}^4$ it results that $\|\mathbf{v}\| \le c\|\mathbf{x}\|_2$, in particular $\|\mathbf{a}^{(g)}\| < c\|\mathbf{a}^{(g)}\|_2 = c$. So,

$$\begin{aligned}&\left\|\left(\vartheta^{(1)}\varphi\left(B(\epsilon)\right)-\vartheta(t_0+T)I\right)\mathbf{a}^{(g)}\right\|\\ &\le c\left\|\vartheta^{(1)}\varphi\left(B(\epsilon)\right)-\vartheta(t_0+T)I\right\|\\ &\le c\left(|\vartheta^{(1)}|\|\varphi\left(B(\epsilon)\right)\|+|\vartheta(t_0+T)|\right)\\ &\le 2c\max\left(|\vartheta^{(1)}|,|\vartheta(t_0+T)|\right).\end{aligned}$$

A.3 Proof of Theorem 4

Since the sensitivity of Δsoc to $Temp^{(1)}$ is defined as $s_{\Delta soc,Temp^{(1)}} = \mathbb{1}^\intercal\mathbf{s}_{\Delta\bar{\mathbf{c}},Temp^{(1)}}$, let us begin by obtaining the initial value problem for $\mathbf{s}_{\Delta\bar{\mathbf{c}},Temp^{(1)}}$. According to Eq. 15, applied to Eq. 17, we have that for all $t\in]t_0+T,t_0+2T]$

$$\begin{aligned}\frac{d\mathbf{s}_{\Delta\bar{\mathbf{c}},Temp^{(1)}}}{dt} &= \rho^{(1)}(r)A\mathbf{s}_{\Delta\bar{\mathbf{c}},Temp^{(1)}}\\ &\quad+\frac{\partial}{\partial Temp^{(1)}}\left(\rho^{(1)}(r)A\Delta\bar{\mathbf{c}}+\vartheta^{(1)}\mathbf{a}^{(g)}\right),\\ \mathbf{s}_{\Delta\bar{\mathbf{c}},Temp^{(1)}}(t_0+T) &= \frac{\partial\Delta\bar{\mathbf{c}}(t_0+T)}{\partial Temp^{(1)}} = \mathbf{0},\end{aligned}\tag{29}$$

where

$$\begin{aligned}&\frac{\partial}{\partial Temp^{(1)}}\left(\rho^{(1)}(r)A\Delta\bar{\mathbf{c}}+\vartheta^{(1)}\mathbf{a}^{(g)}\right)\\ &= \frac{\partial\rho^{(1)}(r)}{\partial Temp^{(1)}}A\Delta\bar{\mathbf{c}}+\frac{\partial\vartheta^{(1)}}{\partial Temp^{(1)}}\mathbf{a}^{(g)}\\ &= \frac{\partial\rho^{(1)}(r)}{\partial Temp^{(1)}}\left(A\Delta\bar{\mathbf{c}}-\frac{\mathbf{a}^{(g)}}{T\rho^{(0)}(r)}\right).\end{aligned}$$

Thus, for all $t\in]t_0+T,t_0+2T]$

$$\begin{aligned}\frac{d\mathbf{s}_{\Delta\bar{\mathbf{c}},Temp^{(1)}}}{dt} &= \rho^{(1)}(r)A\mathbf{s}_{\Delta\bar{\mathbf{c}},Temp^{(1)}}\\ &\quad+\frac{\partial\rho^{(1)}(r)}{\partial Temp^{(1)}}\left(A\Delta\bar{\mathbf{c}}-\frac{\mathbf{a}^{(g)}}{T\rho^{(0)}(r)}\right).\end{aligned}$$

By multiplying both sides of the previous equation by $\mathbb{1}^\intercal$, and by recalling that $\mathbb{1}^\intercal A = -\delta\mathbf{k}^\intercal$, and $\mathbb{1}^\intercal\mathbf{a}^{(g)} = 1$, Eq. 21 is proved.

For proving the second part of the statement, let us consider the expression of $\Delta\bar{\mathbf{c}}(t)$ in Eq. 19.

By setting $\psi(t) := \mathbf{k}^\mathsf{T}\varphi\left(\rho^{(1)}(r)A(t-t_0-T)\right)\mathbf{a}^{(g)}$, we have that

$$\mathbf{k}^\mathsf{T}\Delta\bar{\mathbf{c}}(t) = (t-t_0-T)\psi(t)\vartheta^{(1)},$$

and, by replacing $\vartheta^{(1)}$ with its definition in Eq. 18, Eq. 21 becomes

$$\begin{aligned}\frac{ds_{\Delta soc,Temp^{(1)}}}{dt} &= -\rho^{(1)}(r)\delta\mathbf{k}^\mathsf{T}\mathbf{s}_{\Delta\bar{\mathbf{c}},Temp^{(1)}} \\ &\quad -\frac{\partial\rho^{(1)}(r)}{\partial Temp^{(1)}}\Bigg[\frac{\delta(t-t_0-T)\psi(t)}{T} \\ &\quad \left(N_P^{(1)}-\frac{\rho^{(1)}(r)}{\rho^{(0)}(r)}\right)+\frac{1}{T\rho^{(0)}(r)}\Bigg].\end{aligned}$$

Consider that $\psi(t_0+T) = \mathbf{k}^\mathsf{T}\mathbf{a}^{(g)} > 0$, then, by continuity, there is a number $\bar{\epsilon} > 0$ such that $\psi(t) > 0$ for all $t \in]t_0+T, t_0+T+\bar{\epsilon}]$. By defining $k_{min} := \min_i \mathbf{k}_i$, then $\mathbf{k}^\mathsf{T}\mathbf{s}_{\Delta\bar{\mathbf{c}},Temp^{(1)}} \geq k_{min}\mathbb{1}^\mathsf{T}\mathbf{s}_{\Delta\bar{\mathbf{c}},Temp^{(1)}}$, and $\delta(t-t_0-T)\psi(t)N_P^{(1)} > 0$ for all $t \in]t_0+T, t_0+T+\bar{\epsilon}]$. It follows that

$$\begin{aligned}\frac{ds_{\Delta soc,Temp^{(1)}}}{dt} &\leq -\rho^{(1)}(r)\delta k_{min}\mathbb{1}^\mathsf{T}\mathbf{s}_{\Delta\bar{\mathbf{c}},Temp^{(1)}} \\ &\quad -\frac{\partial\rho^{(1)}(r)}{\partial Temp^{(1)}}\frac{1-\delta(t-t_0-T)\psi(t)\rho^{(1)}(r)}{T\rho^{(0)}(r)}\end{aligned}$$

for all $t \in]t_0+T, t_0+T+\bar{\epsilon}]$.

Notice that the function $(t-t_0-T)\psi(t)$ is positive for all $t \in]t_0+T, t_0+T+\bar{\epsilon}]$ and it is equal to zero at $t = t_0+T$. Since $\dfrac{1}{\delta\rho^{(1)}(r)} > 0$, there exists an $\epsilon > 0$ such that $(t-t_0-T)\psi(t) \leq \dfrac{1}{\delta\rho^{(1)}(r)}$ for all $t \in]t_0+T, t_0+T+\epsilon]$. Thus, exploiting the positivity[5] of $\dfrac{\partial\rho^{(1)}(r)}{\partial Temp^{(1)}}$, we have that

$$\begin{aligned}&\frac{ds_{\Delta soc,Temp^{(1)}}}{dt} \leq -\rho^{(1)}(r)\delta k_{min}\mathbb{1}^\mathsf{T}\mathbf{s}_{\Delta\bar{\mathbf{c}},Temp^{(1)}}, \\ &\forall t \in]t_0+T, t_0+T+\epsilon] \\ &s_{\Delta soc,Temp^{(1)}}(t_0+T) = 0.\end{aligned}$$

The solution of the Cauchy problem $\dfrac{dx}{dt} = -\rho^{(1)}(r)\delta k_{min}x$, with $x(t_0+T) = 0$, is the function $x(t) \equiv 0$, for all $t \in [t_0+T, t_0+T+\epsilon]$. Since $s_{\Delta soc,Temp^{(1)}}(t_0+T) = x(t_0+T) = 0$, we have that $s_{\Delta soc,Temp^{(1)}} \leq x(t) = 0$, for all $t \in [t_0+T, t_0+T+\epsilon]$.

[5] $\dfrac{\partial\rho^{(1)}(r)}{\partial Temp^{(1)}} = \dfrac{106.06}{47.91}(k_a(Temp^{(1)}))^2 k_b(Acc^{(1)})k_c(r)\dfrac{e^{\frac{106.06}{Temp^{(1)}+\frac{106.06}{log(46.91)}-Temp^{(0)}}}}{(Temp^{(1)}+\frac{106.06}{log(46.91)}-Temp^{(0)})^2} > 0.$

A.4 Proof of Theorem 5

At first, let us consider the sensitivity of $\Delta\bar{\mathbf{c}}$ to $N_P^{(1)}$, which satisfies the following initial value problem

$$\begin{aligned}\frac{d\mathbf{s}_{\Delta\bar{\mathbf{c}},N_P^{(1)}}}{dt} &= \rho^{(1)}(r)A\mathbf{s}_{\Delta\bar{\mathbf{c}},N_P^{(1)}}+\frac{\mathbf{a}^{(g)}}{T}, \quad t \in]t_0+T, t_0+2T] \\ \mathbf{s}_{\Delta\bar{\mathbf{c}},N_P^{(1)}}(t_0+T) &= \mathbf{0},\end{aligned} \tag{30}$$

according to Eq. 15 applied to Eq. 17.

By recalling that $\mathbb{1}^\mathsf{T}A = -\delta\mathbf{k}^\mathsf{T}$ and $\mathbb{1}^\mathsf{T}\mathbf{a}^{(g)} = 1$ it is easy to see that $s_{\Delta soc,N_P^{(1)}}$ satisfies the initial value problem (22).

To complete the proof, let us define $k_{max} := \max_i \mathbf{k}_i$. Thus,

$$\frac{ds_{\Delta soc,N_P^{(1)}}}{dt} \geq -\rho^{(1)}(r)\delta k_{max}s_{\Delta soc,N_P^{(1)}},$$

for all $t \in]t_0+T, t_0+2T]$. Since $s_{\Delta soc,N_P^{(1)}}(t_0+T) = 0$, we have that $s_{\Delta soc,N_P^{(1)}} \geq 0$ for all $t \in [t_0+T, t_0+2T]$.

A.5 Proof of Theorem 6

Let us begin by obtaining the initial value problem for $\mathbf{s}_{\Delta\bar{\mathbf{c}},r}$. According to Eqs. 15 applied to Eq. 17, we have that

$$\begin{aligned}\frac{d\mathbf{s}_{\Delta\bar{\mathbf{c}},r}}{dt} &= \rho^{(1)}(r)A\mathbf{s}_{\Delta\bar{\mathbf{c}},r} \\ &\quad +\frac{\partial}{\partial r}\left(\rho^{(1)}(r)A\Delta\bar{\mathbf{c}}+\vartheta^{(1)}\mathbf{a}^{(g)}\right) \\ \mathbf{s}_{\Delta\bar{\mathbf{c}},r}(t_0+T) &= \frac{\partial\Delta\bar{\mathbf{c}}(t_0+T)}{\partial r} = \mathbf{0},\end{aligned} \tag{31}$$

where

$$\begin{aligned}\frac{\partial}{\partial r}\left(\rho^{(1)}(r)A\Delta\bar{\mathbf{c}}+\vartheta^{(1)}\mathbf{a}^{(g)}\right) &= \frac{\partial\rho^{(1)}(r)}{\partial r}A\Delta\bar{\mathbf{c}}+\vartheta^{(1)}\frac{\partial\mathbf{a}^{(g)}}{\partial r} \\ &= \frac{\partial\rho^{(1)}(r)}{\partial r}A\Delta\bar{\mathbf{c}}+\frac{\vartheta^{(1)}}{(r+1)^2}\mathbf{v}\end{aligned}$$

and $\mathbf{v} := [1, -1, 0, 0]^\mathsf{T}$. Thus, we have that

$$\frac{d\mathbf{s}_{\Delta\bar{\mathbf{c}},r}}{dt} = \rho^{(1)}(r)A\mathbf{s}_{\Delta\bar{\mathbf{c}},r}+\frac{\partial\rho^{(1)}(r)}{\partial r}A\Delta\bar{\mathbf{c}}+\frac{\vartheta^{(1)}\mathbf{v}}{(r+1)^2}.$$

By multiplying both sides of the above equation by $\mathbb{1}^\mathsf{T}$, and recalling that $\mathbb{1}^\mathsf{T}A = -\delta\mathbf{k}^\mathsf{T}$, and $\mathbb{1}^\mathsf{T}\mathbf{v} = 0$, Eq. 23 is proved.

For the second part of the proof, as in the proof of Theorem 4, there exists an $\epsilon > 0$ such that for all $t \in]t_0+T, t_0+T+\epsilon]$ the sign of the function

$$\mathbf{k}^\mathsf{T}\Delta\bar{\mathbf{c}}(t) = \vartheta^{(1)}(t-t_0-T)\mathbf{k}^\mathsf{T}\varphi\left(\rho^{(1)}(r)A(t-t_0-T)\right)\mathbf{a}^{(g)}$$

is the same as the sign of $\vartheta^{(1)}$. For this reason, we distinguish the two cases: $\vartheta^{(1)} \geq 0$ and $\vartheta^{(1)} < 0$. Let us observe that $\frac{\partial \rho^{(1)}(r)}{\partial r} > 0$[6] so that, when $\vartheta^{(1)} \geq 0$, it results

$$\frac{ds_{\Delta soc,r}}{dt} = -\rho^{(1)}(r)\delta\mathbf{k}^\mathsf{T}\mathbf{s}_{\Delta\bar{\mathbf{c}},r} - \frac{\partial \rho^{(1)}(r)}{\partial r}\delta\mathbf{k}^\mathsf{T}\Delta\bar{\mathbf{c}}$$
$$\leq -\rho^{(1)}(r)\delta k_{min} s_{\Delta soc,r}.$$

Since $s_{\Delta soc,r}(t_0 + T) = 0$, we have that $s_{\Delta soc,r}(t) \leq 0$ for all $t \in [t_0 + T, t_0 + T + \epsilon]$. If $\vartheta^{(1)} < 0$, then $\frac{ds_{\Delta soc,r}}{dt} \geq -\rho^{(1)}(r)\delta k_{max} s_{\Delta soc,r}$ so that, as $s_{\Delta soc,r}(t_0 + T) = 0$, then $s_{\Delta soc,r}(t_0 + T) \geq 0$, for all $t \in [t_0 + T, t_0 + T + \epsilon]$ and this completes the proof.

A.6 Thornthwaite's formula for estimating the potential evapotranspiration

We need to estimate the potential evapotranspiration $pet(t)$, $[mmmonth^{-1}]$, estimated by means of the Thornthwaite's formula which is expressed, for the nth year, on a monthly basis at the instants $t_m^{(n)} := t_0 + nT + \frac{T}{365}\sum_{i=1}^{m} N_i$ with $m = 1, \ldots, 12$ and N_i denoting the number of days of the ith month of the nth year,[7] as follows:

$$pet(t_m^{(n)}) := 16\frac{L_{d,m}^{(n)}}{12}\frac{N_m}{30}\left(\frac{10Temp_{d,m}^{(n)}}{I_n}\right)^a.$$

In the above formula, $L_{d,m}^{(n)}$ and $Temp_{d,m}^{(n)}$ represent the average day length (hours) and the average daily temperature of the mth month of the nth year, respectively. Finally, I_n is the heat index for the nth year given by

$$I_n = \sum_{k=1}^{12}\left(\frac{Temp_k^{(n)}}{5}\right)^{1.5}$$

where $Temp_k^{(n)} := \frac{\int_{t_{k-1}^{(n)}}^{t_k^{(n)}} Temp(s)ds}{t_k^{(n)} - t_{k-1}^{(n)}}$ is the kth monthly mean temperature, for $k = 1, \ldots, 12$. Finally,

$$a = 6.710^{-7}I_n^3 - 7.710^{-5}I_n^2 + 1.810^{-2}I_n + 0.49.$$

A.7 Estimation of the accumulate soil moisture deficit

The accumulate soil moisture deficit in the nth year, is also estimated on a monthly basis at the instants $t_m^{(n)} := t_0 + nT + \frac{T}{365}\sum_{i=1}^{m} N_i$ with $m = 1, \ldots, 12$. Then $Acc(t_m^{(n)}, M) = 0$ for all $m = 1, \ldots, \bar{m}$ such that $pet(t_m^{(n)}) \leq rain(t_m^{(n)})$, while

$$Acc(t_m^{(n)}, M) = \min\left(\max\left(M, Acc(t_{m-1}^{(n)}, M) + rain(t_m^{(n)}) - pet(t_m^{(n)})\right), 0\right)$$

for $m = \bar{m} + 1, \ldots, 12$.

[6] $\frac{\partial \rho}{\partial r}(Temp^{(1)}, r) = k_a(Temp^{(1)})k_b(Acc^{(1)})N_b\frac{e^{x(r)}}{r^2\left(1+e^{x(r)}\right)^2}$, $x(r) = \frac{30(r-1)}{r}$

[7] In a leap year $t_m^{(n)} := t_0 + nT + \frac{T}{366}\sum_{i=1}^{m} N_i$ and $N_2 = 29$.

Acknowledgements The authors would like to thank the referee for valuable comments which helped to improve the presentation of the results. This study was carried out within the framework of the H2020 project "Earth Observation Training in Science and Technology at the Space Research Centre of the Polish Academy of Sciences"—'EOTiST"'. The project has received funding from the European Union's Horizon 2020 research and innovation programme under grant agreement No 952111. The work of Angela Martiradonna has been carried out within the project "Modelli differenziali per la salvaguardia della biodiversità minacciata dalle specie invasive nelle aree protette. Utilizzo di dati satellitari per l'analisi di scenario e il controllo ottimo nel Parco Nazionale dell'Alta Murgia" funded by "Research for Innovation" (REFIN) progamme n. 0C46E06B- Regione Puglia, Italy.

References

1. Borrelli, L., Colecchia, S., Troccoli, A., Caradonna, S., Papini, R., Ventrella, D., Dell'Abate, M.T., Galeffi, C., Tomasoni, C., Farina, R.: Effectiveness of the gaec standard of cross compliance crop rotations in maintaining organic matter levels in soils. Ital. J. Agron. **6**(s1), e8–e8 (2011)
2. Chenu, C., Angers, D.A., Barré, P., Derrien, D., Arrouays, D., Balesdent, J.: Increasing organic stocks in agricultural soils: Knowledge gaps and potential innovations. Soil Tillage Res. **188**, 41–52 (2019)
3. Coleman, K., Jenkinson, D.: Rothc-26.3—a model for the turnover of carbon in soil. In: Evaluation of Soil Organic Matter Models, pp. 237–246. Springer (1996)
4. Dickinson, R.P., Gelinas, R.J.: Sensitivity analysis of ordinary differential equation systems—a direct method. J. Comput. Phys. **21**(2), 123–143 (1976)
5. Diele, F., Marangi, C., Martiradonna, A.: Non-standard discrete rothc models for soil carbon dynamics. Axioms **10**(2), 56 (2021)
6. Falloon, P., Smith, P., Coleman, K., Marshall, S.: Estimating the size of the inert organic matter pool from total soil organic carbon content for use in the rothamsted carbon model. Soil Biol. Biochem. **30**(8–9), 1207–1211 (1998)

7. Farina, R., Coleman, K., Whitmore, A.P.: Modification of the rothc model for simulations of soil organic c dynamics in dryland regions. Geoderma **200**, 18–30 (2013)
8. Fuglestvedt, J., Rogelj, J., Millar, R.J., Allen, M., Boucher, O., Cain, M., Forster, P.M., Kriegler, E., Shindell, D.: Implications of possible interpretations of 'greenhouse gas balance' in the Paris agreement. Philos. Trans. R. Soc. A: Math. Phys. Eng. Sci. **376**(2119), 20160445 (2018)
9. Gottschalk, P., Smith, J.U., Wattenbach, M., Bellarby, J., Stehfest, E., Arnell, N., Osborn, T., Jones, C., Smith, P.: How will organic carbon stocks in mineral soils evolve under future climate? Global projections using rothc for a range of climate change scenarios. Biogeosciences **9**(8), 3151–3171 (2012)
10. Hammoudi, A., Iosifescu, O., Bernoux, M.: Mathematical analysis of a nonlinear model of soil carbon dynamics. Differ. Equ. Dyn. Syst. **23**(4), 453–466 (2015)
11. Harris, I., Osborn, T.J., Jones, P., Lister, D.: Version 4 of the cru ts monthly high-resolution gridded multivariate climate dataset. Scientific Data **7**(1), 1–18 (2020)
12. Krause, A., Knoke, T., Rammig, A.: A regional assessment of land-based carbon mitigation potentials: bioenergy, beccs, reforestation, and forest management. GCB Bioenergy **12**(5), 346–360 (2020)
13. Lehmann, J., Kleber, M.: The contentious nature of soil organic matter. Nature **528**(7580), 60–68 (2015)
14. Lorenz, K., Lal, R., Ehlers, K.: Soil organic carbon stock as an indicator for monitoring land and soil degradation in relation to united nations' sustainable development goals. Land Degrad. Dev. **30**(7), 824–838 (2019)
15. Minelli, S.: Scientific conceptual framework for land degradation neutrality: a report of the science-policy interface. United Nations Convention to Combat Desertification (UNCCD) (2017)
16. Morais, T.G., Silva, C., Jebari, A., Álvaro-Fuentes, J., Domingos, T., Teixeira, R.F.: A proposal for using process-based soil models for land use life cycle impact assessment: application to Alentejo, Portugal. J. Clean. Prod. **192**, 864–876 (2018)
17. Morais, T.G., Teixeira, R.F., Domingos, T.: Detailed global modelling of soil organic carbon in cropland, grassland and forest soils. Plos One **14**(9), e0222604 (2019)
18. Orr, B., Cowie, A., Castillo Sanchez, V., Chasek, P., Crossman, N., Erlewein, A., Louwagie, G., Maron, M., Metternicht, G., Minelli, S., et al: Scientific conceptual framework for land degradation neutrality. In: A Report of the Science-Policy Interface, pp. 1–98. United Nations Convention to Combat Desertification (UNCCD), Bonn (2017)
19. Parshotam, A.: Modelling recalcitrant soil organic carbon, the "holy grail" in soil science
20. Parshotam, A.: The rothamsted soil-carbon turnover model—discrete to continuous form. Ecol. Model. **86**(2–3), 283–289 (1996)
21. Parshotam, A.: Inert organic matter (iom) in the rothamsted soil carbon turnover model: analytical solutions. Landcare Res. 727–732 (1999)
22. Parton, W.: The century model. In: Evaluation of Soil Organic Matter Models, pp. 283–291. Springer (1996)
23. Running, S., Zhao, M.: Mod17a3hgf modis/terra net primary production gap-filled yearly l4 global 500m sin grid v006. NASA EOSDIS Land Processes DAAC. Available online: https://doi.org/10.5067/MODIS/MOD17A3HGF **6** (2019)
24. Sims, N., Newnham, G., England, J., Guerschman, J., Cox, S., Roxburgh, S., Viscarra Rossel, R.A., Fritz, S., Wheeler, I.: Good Practice Guidance. Sdg Indicator 15.3.1, Proportion of Land that is Degraded over Total Land Area Version 2.0. United Nations Convention to Combat Desertification (UNCCD), Bonn (2021)
25. Smith, J., Smith, P., Wattenbach, M., Zaehle, S., Hiederer, R., Jones, R.J., Montanarella, L., Rounsevell, M.D., Reginster, I., Ewert, F.: Projected changes in mineral soil carbon of european croplands and grasslands, 1990–2080. Glob. Chang. Biol. **11**(12), 2141–2152 (2005)
26. Team, A.: Application for extracting and exploring analysis ready samples (Appeears). Ver. 2.60. In: NASA EOSDIS Land Processes Distributed Active Archive Center (LP DAAC), USGS/Earth Resources Observation and Science (EROS) Center, Sioux Falls, South Dakota, USA (2020)